International Journal of Solids and Structures 45 (2008) 4990–5014

Contents lists available at ScienceDirect

International Journal of Solids and Structures

journal homepage: www.elsevier.com/locate/ijsolstr

Subinterface crack in an anisotropic piezoelectric bimaterial

P.S. Yang [a], J.Y. Liou [b], J.C. Sung [a,*]

[a] Department of Civil Engineering, National Cheng Kung University, No. 1, University Road, Tainan 70101, Taiwan, ROC
[b] Department of Civil Engineering, Kao Yuan University, Kaohsiung 82151, Taiwan, ROC

ARTICLE INFO

Article history:
Received 23 October 2007
Received in revised form 23 April 2008
Available online 9 May 2008

Keywords:
Subinterface crack
Generalized Stroh formalism
Anisotropic piezoelectric materials
Generalized stress intensity factors

ABSTRACT

In this paper, the problem of a subinterface crack in an anisotropic piezoelectric bimaterial is analyzed. A system of singular integral equations is formulated for general anisotropic piezoelectric bimaterial with kernel functions expressed in complex form. For commonly used transversely isotropic piezoelectric materials, the kernel functions are given in real forms. By considering special properties of one of the bimaterial, various real kernel functions for half-plane problems with mechanical traction-free or displacement-fixed boundary conditions combined with different electric boundary conditions are obtained. Investigations of half-plane piezoelectric solids show that, particularly for the mechanical traction-free problem, the evaluations of the *mechanical stress intensity factors* (*electric displacement intensity factor*) under *mechanical* loadings (*electric displacement loading*) for *coupled* mechanical and electric problems may be evaluated directly by considering the corresponding *decoupled elastic* (*electric*) problem irrespective of what electric boundary condition is applied on the boundary. However, for the piezoelectric bimaterial problem, purely elastic bimaterial analysis or purely electric bimaterial analysis is inadequate for the determination of the generalized stress intensity factors. Instead, both elastic and electric properties of the bimaterial's constants should be simultaneously taken into account for better accuracy of the generalized stress intensity factors.

1. Introduction

Wide applications of electromechanical and electronic devices, such as ultrasonic generators, sensors, transducers, and actuators, have motivated research in piezoelectric materials. A better understanding of the intrinsic coupling effect between mechanical and electric fields can provide information to improve the performance of the electromechanical devices. The behaviors of cracks in homogeneous piezoelectric materials have been investigated in great depth, e.g., Gao and Fan (1999), Gao and Wang (1999), Park and Sun (1995), Sosa (1991), and Pak (1990). Cracks in inhomogeneous piezoelectric media have also been widely studied, especially for interface crack problems. The fundamental features of interface cracks have been addressed by Suo et al. (1992) and Ou and Chen (2004). Cracks interacting with the interface between dissimilar piezoelectric materials are also attracting a lot of attention. For example, Tian and Chen (2000) investigated the interaction between a semi-infinite interface and a subinterface microcrack using the pseudo-traction electric displacement method. Beom et al. (2003) investigated a problem similar to that considered by Tian and Chen (2000), but with different loadings prescribed on the far fields. A crack arbitrarily oriented near a perfect interface in piezoelectric bimaterials was considered by Tian and Chau (2003). However, their formulation is not suitable for the special problem of subinterface crack in a *horizontal* orientation relative to the interface. In their investigations of the interactions between subinterface cracks and the interface, Tian and Chen (2002) provided some information for a subinterface *horizontal* crack problem, employing again

* Corresponding author. Tel.: +886 6 2757575; fax: +886 6 2358542.
E-mail address: jcsung@mail.ncku.edu.tw (J.C. Sung).

0020-7683/$ - see front matter
doi:10.1016/j.ijsolstr.2008.05.001

the pseudo-traction electric displacement method. Besides, their attention is restricted to the investigations of the very special metal/piezoelectric bimaterial. The problem of parallel crack near the interface of magnetoelectroelastic bimaterials has been recently studied by Tian and Gabbert (2005). All the studies mentioned above were formulated in terms of integral equations, the kernels of which are expressed generally in complex forms (see Tian and Chen, 2000; Tian and Chau, 2003) where the dependences of the kernel functions on the material constants are not further exploited. It should be noted that when the distance between the subinterface crack and the interface is small compared with the crack length and other dimensions of the problem, the behaviors of crack–interface interactions will become more intriguing. Under certain conditions, one of the crack tips may be closed so that the singular behavior for the stress will change. The correct analysis taken this into account has been done by Xiao and Fan (2001) and Xiao et al. (2000). In the following, we will focus on the problems of cracks not so close to the interface.

In this paper, the problem of a subinterface horizontal crack in an anisotropic piezoelectric bimaterial is analyzed (see Fig. 1), with emphases placed firstly on the development of the real kernel functions for bimaterial (or half-plane) problem and then on the problem of whether the coupled mechanical and electric bimaterial (or half-plane) problem may be analyzed by the corresponding decoupled elastic and dielectric bimaterial (or half-plane) problem. To proceed, the subinterface crack problem is formulated in terms of a system of singular integral equations with the unknown generalized dislocation densities defined on the crack faces. The kernel functions developed are in complex form for general anisotropic piezoelectric bimaterial. For commonly used transversely isotropic piezoelectric bimaterials, the kernel functions are given in *real* forms, as mentioned above. The real kernel functions are decoupled into those kernel functions for elastic bimaterial and electric bimaterial, respectively, when the piezoelectric-stress effects disappear. The kernel functions for the elastic bimaterial problem recover those developed by Sung and Liou (1995b). Moreover, by considering certain special properties of one of the bimaterial, for example the upper un-cracked material, the real kernel functions for half-plane problems with various combinations of mechanical (either traction-free or displacement-fixed) and electric boundary conditions (electric-open, electric-closed, or electric-flux-continuous) are obtained. Analyses show that for half-plane problems with various electric boundary conditions, particularly for mechanical traction-free problem, the evaluations of the *mechanical stress intensity factors* (*electric displacement intensity factor*) under *mechanical* loadings (*electric displacement loading*) for *coupled* mechanical and electric problems may be evaluated directly by considering the corresponding *decoupled elastic* (*electric*) problem irrespective of what electric boundary is applied on the boundary. This was also observed by Yang et al. (2007), but for traction-free and electric-open boundary conditions only. For the piezoelectric bimaterial problem, however, investigations show that purely elastic bimaterial analysis or purely electric bimaterial analysis is inadequate for the determination of the generalized stress intensity factors. Instead, both elastic and electric properties of the bimaterial's constants should be taken into account for better accuracy of the generalized stress intensity factors.

2. Generalized Stroh formalism

In a rectangular coordinate system $x_i (i = 1, 2, 3)$, the basic equations for a linear piezoelectric material (Suo et al., 1992; Ting, 1996) are given by

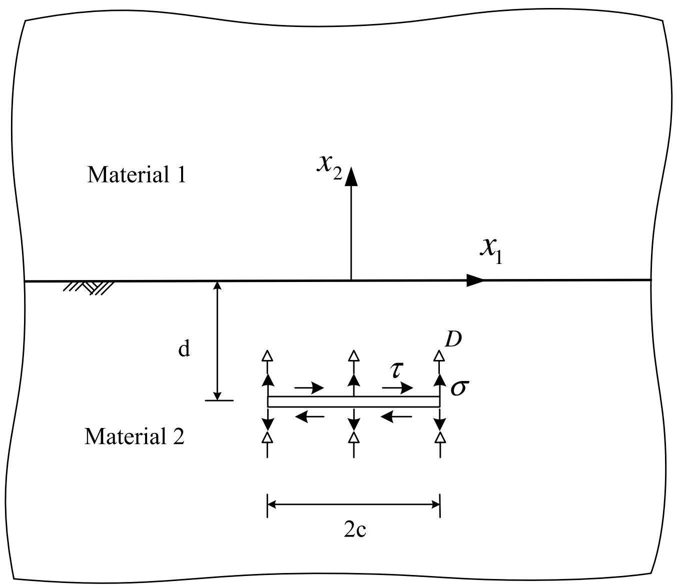

Fig. 1. Geometry of the problem.

$$\sigma_{ij} = c_{ijkl}\varepsilon_{kl} - e_{kij}E_k, \quad D_i = e_{ikl}\varepsilon_{kl} + \alpha_{ik}E_k, \tag{2.1}$$

$$\varepsilon_{ij} = \frac{1}{2}(u_{i,j} + u_{j,i}), \quad E_i = -u_{4,i}, \tag{2.2}$$

$$\sigma_{ij,j} = 0, \quad D_{i,i} = 0, \tag{2.3}$$

where σ_{ij}, ε_{kl}, D_i and E_k are the stresses, the strains, electric displacements and the electric field respectively. u_i (i = 1, 2, 3) and u_4 are the elastic displacements and electric potential, respectively. c_{ijkl}, e_{kij}, and α_{ik} are the elastic stiffness, piezoelectric-stress, and dielectric constants, respectively. Furthermore, these material constants satisfy the following symmetric relationship:

$$c_{ijkl} = c_{jikl} = c_{ijlk} = c_{klij}, \quad e_{kij} = e_{kji}, \quad \alpha_{ik} = \alpha_{ki}. \tag{2.4}$$

For a two-dimensional deformation, where $u_\alpha(\alpha = 1, 2, 3, 4)$ depend on x_1 and x_2 only, the generalized displacement vector $\boldsymbol{u} = [u_1, u_2, u_3, u_4]^{\mathrm{T}}$ and generalized stress function vector $\boldsymbol{\varphi} = [\phi_1, \phi_2, \phi_3, \phi_4]^{\mathrm{T}}$ can be expressed as

$$\boldsymbol{u} = 2\mathrm{Re}\{\boldsymbol{Af}(\boldsymbol{z})\}, \tag{2.5}$$

$$\boldsymbol{\varphi} = 2\mathrm{Re}\{\boldsymbol{Bf}(\boldsymbol{z})\}, \tag{2.6}$$

where

$$\boldsymbol{A} = [\boldsymbol{a}_1, \boldsymbol{a}_2, \boldsymbol{a}_3, \boldsymbol{a}_4], \quad \boldsymbol{B} = [\boldsymbol{b}_1, \boldsymbol{b}_2, \boldsymbol{b}_3, \boldsymbol{b}_4], \tag{2.7}$$

$$\boldsymbol{f}(\boldsymbol{z}) = [f_1(z_1), f_2(z_2), f_3(z_3), f_4(z_4)]^{\mathrm{T}}, \tag{2.8}$$

$$z_\alpha = x_1 + p_\alpha x_2, \quad (\alpha = 1, 2, 3, 4), \tag{2.9}$$

where the superscript T indicates transposition and $f_\alpha(z_\alpha)$, (α = 1, 2, 3, 4) are arbitrary analytic functions of z_α. Column vectors of matrix $\boldsymbol{A}$, i.e., $\boldsymbol{a}_\alpha(\alpha = 1, 2, 3, 4)$ and p_α (α = 1, 2, 3, 4), are determined using the following eigenrelation:

$$\boldsymbol{W}\boldsymbol{a}_\alpha = \boldsymbol{0}, \tag{2.10}$$

where

$$\boldsymbol{W} = [\boldsymbol{Q} + p_\alpha(\boldsymbol{R} + \boldsymbol{R}^{\mathrm{T}}) + p_\alpha^2\boldsymbol{T}], \tag{2.11}$$

$$\boldsymbol{Q} = \begin{bmatrix} c_{i1k1} & e_{1i1} \\ e_{1k1}^{\mathrm{T}} & -\alpha_{11} \end{bmatrix}, \quad \boldsymbol{R} = \begin{bmatrix} c_{i1k2} & e_{1i2} \\ e_{2k1}^{\mathrm{T}} & -\alpha_{12} \end{bmatrix}, \quad \boldsymbol{T} = \begin{bmatrix} c_{i2k2} & e_{2i2} \\ e_{2k2}^{\mathrm{T}} & -\alpha_{22} \end{bmatrix}. \tag{2.12}$$

Note that matrices $\boldsymbol{Q}$, $\boldsymbol{R}$, and $\boldsymbol{T}$ are all 4×4 and the assumption of the positive definite for the materials leads to the symmetric and non-singular properties for matrices $\boldsymbol{Q}$ and $\boldsymbol{T}$. Matrix $\boldsymbol{B}$ in Eq. (2.7) is related to matrix $\boldsymbol{A}$ in the following relationship:

$$\boldsymbol{B} = \boldsymbol{R}^{\mathrm{T}}\boldsymbol{A} + \boldsymbol{TAP}, \tag{2.13}$$

where

$$\boldsymbol{P} = \mathrm{diag}[p_1, p_2, p_3, p_4]. \tag{2.14}$$

The generalized stress function vector expressed in Eq. (2.6) may be employed to evaluate the generalized stress vectors $\boldsymbol{t}_1 = [\sigma_{11}, \sigma_{12}, \sigma_{13}, D_1]^{\mathrm{T}}$ and $\boldsymbol{t}_2 = [\sigma_{21}, \sigma_{22}, \sigma_{23}, D_2]^{\mathrm{T}}$, which is

$$\boldsymbol{t}_1 = -\boldsymbol{\varphi}_{,2}, \quad \boldsymbol{t}_2 = \boldsymbol{\varphi}_{,1}. \tag{2.15}$$

3. Formulation of the problem

The problem considered is shown in Fig. 1. A half-plane anisotropic piezoelectric material (called material 2 or lower material) is bonded perfectly along the interface to another half-plane anisotropic piezoelectric material (called material 1 or upper material). A subinterface crack of length $2c$ is situated in material 2 with a distance d from the interface. The crack faces are subjected to prescribed loads, either mechanical or electric. Following the suggestions of Wang and Mai (2004) and Ueda (2007), the electric impermeable boundary conditions on the crack faces are assumed in our analysis. It is well known that this problem can be formulated in terms of a system of singular integral equations where the unknown functions in the equations are the densities of the generalized dislocations distributed on the crack faces. The kernels of the equations are related to the fundamental solutions due to a generalized dislocation with the generalized Burgers vector $\boldsymbol{b}^* = [b_1^*, b_2^*, b_3^*, b_4^*]^{\mathrm{T}}$(here, $b_i^*(i = 1, 2, 3)$ and b_4^* are mechanical displacement jumps and an electric potential jump in the plane, respectively) applied at point $\boldsymbol{x}^D = (x_1^D, x_2^D)$ with $x_2^D < 0$ in a crack-free piezoelectric bimaterial solid. The fundamental solution for material 2 is (Qin and Zhang, 2000)

$$\boldsymbol{\varphi}^{(2)} = \frac{1}{\pi}\mathrm{Im}\left\{\boldsymbol{B}^{(2)} < \ell n(z_\alpha^{(2)} - z_\alpha^{D^{(2)}}) > \boldsymbol{B}^{(2)^{\mathrm{T}}}\boldsymbol{b}^* + \sum_{\beta=1}^{4}\boldsymbol{B}^{(2)} < \ell n(z_\alpha^{(2)} - \bar{z}_\beta^{D^{(2)}}) > \boldsymbol{B}^{(2)^{-1}}\boldsymbol{F}\overline{\boldsymbol{B}}^{(2)}\boldsymbol{I}_\beta\overline{\boldsymbol{B}}^{(2)^{\mathrm{T}}}\boldsymbol{b}^*\right\}, \tag{3.1}$$

where $\boldsymbol{\varphi}^{(2)}$ is the complex generalized stress function for material 2 and

$$<\ell n(z_\alpha^{(2)} - z_\alpha^{D^{(2)}}) >= \mathrm{diag}\left[\ell n(z_1^{(2)} - z_1^{D^{(2)}}), \ell n(z_2^{(2)} - z_2^{D^{(2)}}), \ell n(z_3^{(2)} - z_3^{D^{(2)}}), \ell n(z_4^{(2)} - z_4^{D^{(2)}})\right], \tag{3.2}$$

$$<\ell n(z_\alpha^{(2)} - \bar{z}_\beta^{D^{(2)}}) >= \mathrm{diag}\left[\ell n(z_1^{(2)} - \bar{z}_\beta^{D^{(2)}}), \ell n(z_2^{(2)} - \bar{z}_\beta^{D^{(2)}}), \ell n(z_3^{(2)} - \bar{z}_\beta^{D^{(2)}}), \ell n(z_4^{(2)} - \bar{z}_\beta^{D^{(2)}})\right], \tag{3.3}$$

$$\boldsymbol{I}_1 = \mathrm{diag}[1,0,0,0], \quad \boldsymbol{I}_2 = \mathrm{diag}[0,1,0,0], \quad \boldsymbol{I}_3 = \mathrm{diag}[0,0,1,0], \quad \boldsymbol{I}_4 = \mathrm{diag}[0,0,0,1], \tag{3.4}$$

$$z_\alpha^{(2)} = x_1 + p_\alpha^{(2)} x_2 (\text{for } x_2 < 0), \quad z_\alpha^{D^{(2)}} = x_1^D + p_\alpha^{(2)} x_2^D, \quad (\alpha = 1,2,3,4), \tag{3.5}$$

and matrix $\boldsymbol{F}$ is defined by

$$\boldsymbol{F} = (\overline{\boldsymbol{M}}^{(1)^{-1}} + \boldsymbol{M}^{(2)^{-1}})^{-1} (\overline{\boldsymbol{M}}^{(1)^{-1}} - \overline{\boldsymbol{M}}^{(2)^{-1}}), \tag{3.6}$$

where

$$\boldsymbol{M}^{(j)} = \boldsymbol{L}^{(j)^{-1}} - i\boldsymbol{S}^{(j)} \boldsymbol{L}^{(j)^{-1}}, \quad (j = 1,2). \tag{3.7}$$

Here and in what follows, the superscripts (1) and (2) denote material 1 and 2, respectively. $\boldsymbol{L}^{(j)}$ and $\boldsymbol{S}^{(j)} (j = 1, 2)$ are the generalized Barnett–Lothe tensors (Ting, 1996) defined as

$$\boldsymbol{L}^{(j)} = -2i\boldsymbol{B}^{(j)} \boldsymbol{B}^{(j)^{\mathrm{T}}}, \quad \boldsymbol{S}^{(j)} = i(2\boldsymbol{A}^{(j)} \boldsymbol{B}^{(j)^{\mathrm{T}}} - \boldsymbol{I}), \tag{3.8}$$

where $i^2 = -1$ and $\boldsymbol{I}$ is a 4×4 unit real matrix. Now suppose that there are generalized dislocations with densities $\boldsymbol{b}^*(t)$ distributed over the crack faces. Then, by summing up the generalized tractions $\boldsymbol{t}_2^*$ induced by these generalized dislocation densities on the crack faces, a representation equation for the total generalized tractions on the crack faces can be obtained. For the present problem, the total generalized tractions on the crack faces are known a priori, therefore, a system of singular integral equations is obtained, instead. By expressing variables $z_\alpha^{(2)}$ and $z_\alpha^{D^{(2)}}$ on the crack faces in terms of the new variables ξ and t, respectively, as

$$z_\alpha^{(2)} = \xi - p_\alpha^{(2)} d, \quad |\xi| \leqslant c \tag{3.9}$$

$$z_\alpha^{D^{(2)}} = t - p_\alpha^{(2)} d, \quad |t| \leqslant c(\alpha = 1,2,3,4), \tag{3.10}$$

and then by employing the procedures described above, a system of singular integral equations can be obtained as

$$\frac{-1}{2\pi}\left\{\int_{-c}^{c} \frac{\boldsymbol{v}(t)}{t-\xi} \mathrm{d}t + \int_{-c}^{c} \boldsymbol{K}(\xi,t)\boldsymbol{v}(t)\mathrm{d}t\right\} = \boldsymbol{t}_2^*(\xi), \quad |\xi| \leqslant c, \tag{3.11}$$

where $\boldsymbol{t}_2^*$ is the known traction prescribed on the crack faces and $\boldsymbol{v}(t) = [v_1(t), v_2(t), v_3(t), v_4(t)]^{\mathrm{T}} = \boldsymbol{L}^{(2)} \boldsymbol{b}^*(t)$. The kernel functions $\boldsymbol{K}(\xi, t)$ in Eq. (3.11) are given by

$$\boldsymbol{K}(\xi,t) = \sum_{\beta=1}^{4} \mathrm{Re}\{\boldsymbol{B}^{(2)} \boldsymbol{Z}_\beta \boldsymbol{B}^{(2)^{-1}} \boldsymbol{F} \overline{\boldsymbol{B}}^{(2)} \boldsymbol{I}_\beta \overline{\boldsymbol{B}}^{(2)^{-1}}\}, \tag{3.12}$$

where

$$\boldsymbol{Z}_\beta = \mathrm{diag}\left[\frac{1}{z_1^{(2)} - \bar{z}_\beta^{D^{(2)}}}, \frac{1}{z_2^{(2)} - \bar{z}_\beta^{D^{(2)}}}, \frac{1}{z_3^{(2)} - \bar{z}_\beta^{D^{(2)}}}, \frac{1}{z_4^{(2)} - \bar{z}_\beta^{D^{(2)}}}\right]. \tag{3.13}$$

For single values of generalized displacements around a closed contour surrounding the whole crack, the following auxiliary condition has to be satisfied:

$$\int_{-c}^{c} \boldsymbol{v}(t)\mathrm{d}t = \boldsymbol{0}. \tag{3.14}$$

The coupled singular integral equations for the generalized dislocation densities in Eq. (3.11) combined with Eq. (3.14) can be solved numerically. Once the generalized dislocation densities have been found, the generalized stress intensity factors at the crack tips, i.e., the three stress intensity factors k_{I}, k_{II}, and k_{III} and the electric displacement intensity factor k_{D}, can be extracted directly. For example, for the crack-tip at $\xi = c$, the generalized stress intensity factors are given by (Sung and Liou, 1995a)

$$\boldsymbol{k} = [k_{\mathrm{II}}, k_{\mathrm{I}}, k_{\mathrm{III}}, k_{\mathrm{D}}] = \sqrt{\frac{\pi}{4c}} \boldsymbol{v}^*(c), \tag{3.15}$$

where

$$\boldsymbol{v}^*(c) = \lim_{t \to c} \sqrt{c^2 - t^2} \boldsymbol{v}(t). \tag{3.16}$$

For general anisotropic piezoelectric materials, the determination of the generalized dislocation density $\boldsymbol{v}(t)$ involves the evaluation of matrices $\boldsymbol{F}$ and $\boldsymbol{B}^{(2)}$ since both matrices appear in the kernel functions, as shown in Eq. (3.12). The effects of the piezoelectric material properties on the kernel functions are mostly contained in matrices $\boldsymbol{F}$ and $\boldsymbol{B}^{(2)}$, therefore, it is of interest to express matrices $\boldsymbol{F}$ and $\boldsymbol{B}^{(2)}$ explicitly in terms of material constants. Note that the influence of all the upper material's constants on the behavior of the subinterface crack embedded in the lower material is completely through matrix $\boldsymbol{F}$. Since matrix $\boldsymbol{B}^{(2)}$and the three Barnett–Lothe tensors, two of which are related to the determination of matrix $\boldsymbol{F}$, have been expressed explicitly in terms of material constants by Liou and Sung (2007) for monoclinic piezoelectric materials, the kernel functions originally expressed in complex form for general anisotropic piezoelectric materials may then be expressed in real form for monoclinic piezoelectric materials using their results. In the next section, however, only the results for transversely isotropic piezoelectric materials are presented. We show that the obtained real kernel functions are even valid for *degenerated isotropic materials* which are not applicable if the kernel functions are expressed in complex form, as in Eq. (3.12). This is because matrix $\boldsymbol{B}^{(2)}$ is singular for degenerated isotropic materials.

4. Explicit real kernel functions

As mentioned in the previous section, for general anisotropic piezoelectric materials, the kernel functions are related to matrices $\boldsymbol{F}$ and $\boldsymbol{B}^{(2)}$, both of which are completely determined by the material constants. The explicit forms of matrices $\boldsymbol{F}$and $\boldsymbol{B}^{(2)}$ may be expressed in terms of elastic stiffness (Liou and Sung, 2007). In this section, we briefly outline the required results for the development of the explicit form of the kernel functions for transversely isotropic piezoelectric materials. For transversely isotropic piezoelectric materials with the x_2-axis parallel to the poling direction, the constitutive equations (Eq. (2.1)) are expressed as

$$\begin{bmatrix} \boldsymbol{\sigma} \\ \boldsymbol{D} \end{bmatrix} = \begin{bmatrix} \boldsymbol{c} & \boldsymbol{e} \\ \boldsymbol{e}^{\mathrm{T}} & \boldsymbol{\alpha} \end{bmatrix} \begin{bmatrix} \boldsymbol{\varepsilon} \\ \boldsymbol{E} \end{bmatrix}, \tag{4.1}$$

where

$$\boldsymbol{\sigma} = [\sigma_{11} \quad \sigma_{22} \quad \sigma_{33} \quad \sigma_{23} \quad \sigma_{31} \quad \sigma_{12}]^{\mathrm{T}}, \quad \boldsymbol{D} = [D_1 \quad D_2 \quad D_3]^{\mathrm{T}}, \tag{4.2}$$

$$\boldsymbol{\varepsilon} = [\varepsilon_{11} \quad \varepsilon_{22} \quad \varepsilon_{33} \quad 2\varepsilon_{23} \quad 2\varepsilon_{31} \quad 2\varepsilon_{12}]^{\mathrm{T}}, \quad \boldsymbol{E} = [-E_1 \quad -E_2 \quad -E_3]^{\mathrm{T}},$$

$$\boldsymbol{c} = \begin{bmatrix} c_{11} & c_{12} & c_{13} & 0 & 0 & 0 \\ c_{12} & c_{22} & c_{12} & 0 & 0 & 0 \\ c_{13} & c_{12} & c_{11} & 0 & 0 & 0 \\ 0 & 0 & 0 & c_{44} & 0 & 0 \\ 0 & 0 & 0 & 0 & c_{55} & 0 \\ 0 & 0 & 0 & 0 & 0 & c_{44} \end{bmatrix}, \quad \boldsymbol{e} = \begin{bmatrix} 0 & e_{21} & 0 \\ 0 & e_{22} & 0 \\ 0 & e_{21} & 0 \\ 0 & 0 & e_{16} \\ 0 & 0 & 0 \\ e_{16} & 0 & 0 \end{bmatrix},$$

$$\boldsymbol{\alpha} = \begin{bmatrix} -\alpha_{11} & 0 & 0 \\ 0 & -\alpha_{22} & 0 \\ 0 & 0 & -\alpha_{11} \end{bmatrix},$$

where contracted notations $e_{i\alpha}$ and $c_{\alpha\beta}$ (α, β = 1, 2, ..., 6) are used here for e_{ikl} and c_{ijkl}, respectively. For transversely isotropic piezoelectric materials, matrix $\boldsymbol{W}$ defined in Eq. (2.11) simplifies to

$$\boldsymbol{W} = \begin{bmatrix} (c_{44}p^2 + c_{11}) & (c_{12} + c_{44})p & 0 & (e_{21} + e_{16})p \\ (c_{12} + c_{44})p & (c_{22}p^2 + c_{44}) & 0 & (e_{22}p^2 + e_{16}) \\ 0 & 0 & (c_{44}p^2 + c_{55}) & 0 \\ (e_{21} + e_{16})p & (e_{22}p^2 + e_{16}) & 0 & -(\alpha_{22}p^2 + \alpha_{11}) \end{bmatrix}, \tag{4.3}$$

where $c_{55} = (c_{11} - c_{13})/2$. It is noted that the roots $p_\alpha(\alpha = 1, 2, 3, 4)$ corresponding to $|\boldsymbol{W}| = 0$ for transversely isotropic piezoelectric materials can be classified into two types (Suo et al., 1992). The type I roots

$$p_1 = in_1, \quad p_2 = in_2, \quad p_3 = i\sqrt{c_{55}/c_{44}}, \quad p_4 = in_4, \tag{4.4}$$

are all purely imaginary. Of the type II roots

$$p_1 = m_1 + in_1, \quad p_2 = -m_1 + in_1, \quad p_3 = i\sqrt{c_{55}/c_{44}}, \quad p_4 = in_4, \tag{4.5}$$

two (p_3 and p_4) are purely imaginary and the other two (p_1 and p_2) have non-zero real parts but with equal imaginary parts. Since the anti-plane mechanical deformation is entirely decoupled from both in-plane mechanical deformation and the electric field for transversely isotropic piezoelectric materials, we ignore the anti-plane mechanical deformation hereafter. With this consideration in mind, the sizes of matrices $\boldsymbol{M}^{(j)}$ (j = 1, 2), $\boldsymbol{F}$, and $\boldsymbol{B}^{(j)}$(j = 1, 2) all become 3 × 3 and the roots $p_4^{(j)}(j = 1, 2)$ are relabeled as $p_3^{(j)}(j = 1, 2)$. For both types of roots, the elements of $\boldsymbol{B}^{(j)}$(j = 1, 2) can be constructed as (Liou and Sung, 2007)

$$\boldsymbol{B}^{(j)} = \begin{bmatrix} -p_1^{(j)} & -p_2^{(j)} & -p_3^{(j)}\lambda_3^{(j)} \\ 1 & 1 & \lambda_3^{(j)} \\ -\lambda_1^{(j)} & -\lambda_2^{(j)} & 1 \end{bmatrix}, \quad j = 1, 2, \tag{4.6}$$

where $\lambda_\alpha^{(j)}(\alpha = 1,2,3)$, related to material constants, are listed in Appendix A. Matrices $\boldsymbol{L}^{(j)^{-1}}$ and $\boldsymbol{S}^{(j)}\boldsymbol{L}^{(j)^{-1}}$ $(j = 1,2)$, which are related to $\boldsymbol{M}^{(j)}$ (j = 1, 2), may also be constructed as (Liou and Sung, 2007)

$$\boldsymbol{L}^{(j)^{-1}} = \begin{bmatrix} Y_{11}^{(j)} & 0 & 0 \\ 0 & Y_{22}^{(j)} & Y_{23}^{(j)} \\ 0 & Y_{23}^{(j)} & Y_{33}^{(j)} \end{bmatrix}, \quad \boldsymbol{S}^{(j)}\boldsymbol{L}^{(j)^{-1}} = \begin{bmatrix} 0 & -\widehat{Y}_{12}^{(j)} & -\widehat{Y}_{13}^{(j)} \\ \widehat{Y}_{12}^{(j)} & 0 & 0 \\ \widehat{Y}_{13}^{(j)} & 0 & 0 \end{bmatrix}, \quad j = 1,2, \tag{4.7}$$

where $Y_{\alpha\beta}^{(j)}$ and $\widehat{Y}_{\alpha\beta}^{(j)}$ (α, β = 1, 2, 3) are listed in Appendix B. With the matrices shown in Eq. (4.7), matrix $\boldsymbol{F}$ defined in Eq. (3.6) may be obtained simply using matrix algebraic operations. The final form of $\boldsymbol{F}$ may be arranged as follows:

$$\boldsymbol{F} = \begin{bmatrix} F_{11} & iF_{12} & iF_{13} \\ iF_{21} & F_{22} & F_{23} \\ iF_{31} & F_{32} & F_{33} \end{bmatrix}, \tag{4.8}$$

where all elements of $\boldsymbol{F}$ are in general not zero for bimaterial problems. Although not shown here, these elements are simply certain combinations of $Y_{\alpha\beta}^{(j)}$ and $\widehat{Y}_{\alpha\beta}^{(j)}$ (α, β = 1, 2, 3). For some special bimaterials discussed below, however, elements of $\boldsymbol{F}$ will be given explicitly for the purpose of discussion. Let us first consider kernel functions for which the properties of the lower material belong to type I roots. For type I roots, the elements of $\lambda_\alpha^{(2)}(\alpha = 1,2,3)$ defined in Appendix A for lower material all are real, therefore, matrix $\boldsymbol{B}^{(2)}$ becomes

$$\boldsymbol{B}^{(2)} = \begin{bmatrix} -in_1^{(2)} & -in_2^{(2)} & -in_3^{(2)}\lambda_3^{(2)} \\ 1 & 1 & \lambda_3^{(2)} \\ -\lambda_1^{(2)} & -\lambda_2^{(2)} & 1 \end{bmatrix}. \tag{4.9}$$

The expressions of the real part and imaginary part of the elements of the functions $\boldsymbol{Z}_\beta$ are also needed since $\boldsymbol{Z}_\beta$ appears in the kernel functions in Eq. (3.12). They are expressed as follows:

$$\begin{aligned} r_{\alpha\beta} &= \mathrm{Re}\{1/(z_\alpha^{(2)} - \bar{z}_\beta^{D^{(2)}})\} = (\xi - t)/\Delta_{\alpha\beta}, \\ q_{\alpha\beta} &= \mathrm{Im}\{1/(z_\alpha^{(2)} - \bar{z}_\beta^{D^{(2)}})\} = d(N_{\alpha\beta} + N_{\beta\alpha})/\Delta_{\alpha\beta}, \quad (\alpha, \beta = 1,2,3 \text{ no sum on } \alpha \text{and } \beta) \end{aligned} \tag{4.10}$$

where

$$\Delta_{\alpha\beta} = (\xi - t)^2\widehat{I}_{\alpha\beta} + d^2(N_{\alpha\beta} + N_{\beta\alpha})^2, \tag{4.11a}$$

$$[\widehat{I}_{\alpha\beta}] = \begin{bmatrix} 1 & 1 & 1 \\ 1 & 1 & 1 \\ 1 & 1 & 1 \end{bmatrix}, \quad [N_{\alpha\beta}] = \begin{bmatrix} n_1^{(2)} & n_1^{(2)} & n_1^{(2)} \\ n_2^{(2)} & n_2^{(2)} & n_2^{(2)} \\ n_3^{(2)} & n_3^{(2)} & n_3^{(2)} \end{bmatrix}. \tag{4.11b}$$

Substituting Eqs. (4.9) and (4.10) into Eq. (3.12), the kernel functions for lower material whose roots belong to type I are expressed in real form as

$$\boldsymbol{K}(\xi, t) = \frac{1}{\widehat{B}_1^{(2)^2}} \sum_{j=1}^{3} \begin{bmatrix} K_j^{11} & K_j^{12} & K_j^{13} \\ K_j^{21} & K_j^{22} & K_j^{23} \\ K_j^{31} & K_j^{32} & K_j^{33} \end{bmatrix}, \tag{4.12}$$

where $\widehat{B}_1^{(2)} = \lambda_1^{(2)}\lambda_3^{(2)}(n_2^{(2)} - n_3^{(2)}) + \lambda_2^{(2)}\lambda_3^{(2)}(n_3^{(2)} - n_1^{(2)}) + (n_2^{(2)} - n_1^{(2)})$. Explicit expressions of all the elements in Eq. (4.12) are shown in Appendix C. Note that the type of roots the upper material has is reflected in matrix $\boldsymbol{F}$. It is found that no element of the kernel functions is zero for the subinterface crack problem, implying that there are generally mechanical and electric coupling effects for the subinterface crack problem.

Now let us consider the kernel functions for the lower material whose roots belong to type II. Let

$$\lambda_1^{(2)} = \hat{r} + i\hat{q}, \tag{4.13}$$

where $\hat{r}$ and $\hat{q}$ are the real and imaginary part of $\lambda_1^{(2)}$, respectively. By employing the identities $\lambda_2^{(2)} = \bar{\lambda}_1^{(2)}$ (Eq. (A.1)) and $\mathrm{Im}\{\lambda_3^{(2)}\} = 0$ (Eq. (A.2)) which were implied by the properties of type II roots, i.e., $p_2^{(2)} = -\bar{p}_1^{(2)}$ and $p_3^{(2)} = in_3^{(2)}$ (Eq. (4.5)), matrix $\boldsymbol{B}^{(2)}$ may be expressed as

$$\boldsymbol{B}^{(2)} = \begin{bmatrix} -m_1^{(2)} - in_1^{(2)} & m_1^{(2)} - in_1^{(2)} & -in_3^{(2)}\lambda_3^{(2)} \\ 1 & 1 & \lambda_3^{(2)} \\ -\hat{r} - i\hat{q} & -\hat{r} + i\hat{q} & 1 \end{bmatrix}. \tag{4.14}$$

With matrix $\boldsymbol{B}^{(2)}$expressed as above, and with the real part $r_{\alpha\beta}$ and imaginary part $q_{\alpha\beta}$ of the elements of the functions $\boldsymbol{Z}_\beta$ for type II roots given below

$$
\begin{aligned}
&r_{11} = r_{22} = (\xi - t)/\left[(\xi - t)^2 + 4n_1^{(2)^2} d^2\right],\\
&r_{21} = (\xi - t + 2m_1^{(2)} d)/\left[(\xi - t + 2m_1^{(2)} d)^2 + 4n_1^{(2)^2} d^2\right],\\
&r_{31} = r_{23} = (\xi - t + m_1^{(2)} d)/\left\{(\xi - t)^2 + 2m_1^{(2)} d(\xi - t) + d^2\left[m_1^{(2)^2} + (n_1^{(2)} + n_3^{(2)})^2\right]\right\},\\
&r_{12} = (\xi - t - 2m_1^{(2)} d)/\left[(t - \xi + 2m_1^{(2)} d)^2 + 4n_1^{(2)^2} d^2\right],\\
&r_{32} = r_{13} = (\xi - t - m_1^{(2)} d)/\left\{(\xi - t)^2 - 2m_1^{(2)} d(\xi - t) + d^2\left[m_1^{(2)^2} + (n_1^{(2)} + n_3^{(2)})^2\right]\right\},\\
&r_{33} = (\xi - t)/\left[(\xi - t)^2 + 4n_3^{(2)^2} d^2\right],\\
&q_{11} = q_{22} = 2n_1^{(2)} d/\left[(\xi - t)^2 + 4n_1^{(2)} d^2\right],\\
&q_{21} = 2n_1^{(2)} d/\left[(\xi - t + 2m_1^{(2)} d)^2 + 4n_1^{(2)^2} d^2\right],\\
&q_{31} = q_{23} = d(n_1^{(2)} + n_3^{(2)})/\left\{(\xi - t)^2 + 2m_1^{(2)} d(\xi - t) + d^2\left[m_1^{(2)^2} + (n_1^{(2)} + n_3^{(2)})^2\right]\right\},\\
&q_{12} = 2n_1^{(2)} d/\left[(t - \xi + 2m_1^{(2)} d)^2 + 4n_1^{(2)^2} d^2\right],\\
&q_{32} = q_{13} = d(n_1^{(2)} + n_3^{(2)})/\left\{(\xi - t)^2 + 2m_1^{(2)} d(t - \xi) + d^2\left[m_1^{(2)^2} + (n_1^{(2)} + n_3^{(2)})^2\right]\right\},\\
&q_{33} = 2n_3^{(2)} d/\left[(\xi - t)^2 + 4n_3^{(2)} d^2\right],
\end{aligned}
\tag{4.15}
$$

the real kernel functions for lower material whose roots belong to the type II are obtained as

$$
\boldsymbol{K}(\xi, t) = \frac{1}{\widehat{B}_{\mathrm{II}}^{(2)^2}} \sum_{j=1}^{3} \begin{bmatrix} K_j^{11} & K_j^{12} & K_j^{13} \\ K_j^{21} & K_j^{22} & K_j^{23} \\ K_j^{31} & K_j^{32} & K_j^{33} \end{bmatrix}, \tag{4.16}
$$

where $\widehat{B}_{\mathrm{II}}^{(2)} = -2(m_1^{(2)} + n_1^{(2)}\hat{q}\lambda_3^{(2)} + m_1^{(2)}\hat{r}\lambda_3^{(2)} - n_3^{(2)}\hat{q}_3^{(2)}\lambda_3^{(2)})$. The explicit expressions of all the elements in Eq. (4.16) are listed in Appendix D. Note again that the type of the roots the upper material has is reflected in matrix $\boldsymbol{F}$. Similar to the case for type I roots, no element of the kernel functions is zero for type II roots for the subinterface crack problem.

4.1. Kernel functions for special upper materials

The real kernel functions developed above are for a piezoelectric material occupying the lower half-plane region jointed to another piezoelectric material occupying the upper half-plane region. Kernel functions expressed in general forms may be simplified if the special material in either the upper or lower half-plane is considered. For example, there are mathematically eight possible cases to be considered for the upper material (see the chart drawn below). Among these cases, however, only five meaningful cases, denoted by capital letters from A to E, are discussed in what follows.

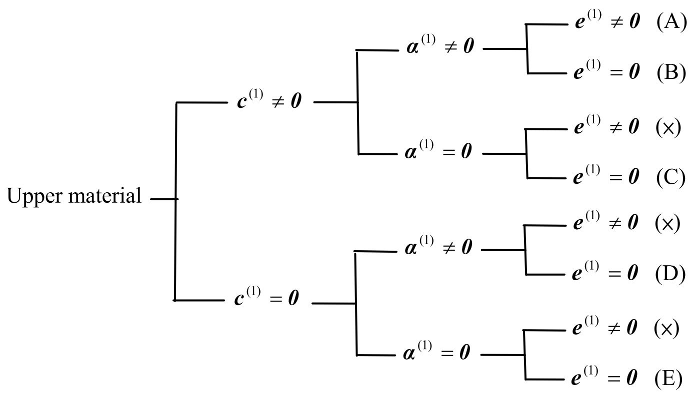

Similarly, there are five cases for the lower half-plane material. In this subsection, we discuss the kernel functions corresponding to the special bimaterials composed of a lower half-plane material, with its property always remaining in case A, i.e., $\boldsymbol{c}^{(2)} \neq \boldsymbol{0}$, $\boldsymbol{\alpha}^{(2)} \neq \boldsymbol{0}$ and $\boldsymbol{e}^{(2)} \neq \boldsymbol{0}$ jointed to an upper half-plane material, with its property varying from case A to case E. Therefore, there are five bimaterials to be discussed below, i.e., (A–A), (A–B), (A–C), (A–D), (A–E), each one with its own special constituent. It should be emphasized again that for all these five bimaterials, the entering of the upper half-plane material's properties into the kernel functions is only through matrix $\boldsymbol{F}$, as can be seen from Eq. (3.6). Therefore the whole structure of the kernel functions corresponding to these five bimaterials is not altered except that the contents of matrix $\boldsymbol{F}$ will take different values for the different cases assumed for the upper material (i.e., cases A–E). The different contents of matrix $\boldsymbol{F}$ for these five bimaterials are discussed below.

(I) Bimaterial (A–A): a lower piezoelectric material jointed to an upper piezoelectric material with $\mathbf{c}^{(1)} \neq \mathbf{0}$, $\boldsymbol{\alpha}^{(1)} \neq \mathbf{0}$ *and* $\mathbf{e}^{(1)} \neq \mathbf{0}$.

This is the general case discussed above, where matrix $\mathbf{F}$ is given by Eq. (4.8).

(II) Bimaterial (A–B): a lower piezoelectric material jointed to an upper elastic-electric decoupled material with $\mathbf{c}^{(1)} \neq \mathbf{0}$, $\boldsymbol{\alpha}^{(1)} \neq \mathbf{0}$ *and* $\mathbf{e}^{(1)} = \mathbf{0}$.

The upper material with the property $\mathbf{c}^{(1)} \neq \mathbf{0}$, $\boldsymbol{\alpha}^{(1)} \neq \mathbf{0}$ and $\mathbf{e}^{(1)} = \mathbf{0}$ signifies that the coupling effect between mechanical and electric fields vanishes since $\mathbf{e}^{(1)} = \mathbf{0}$. Here, we call such a material an *"elastic-electric decoupled material"*. In this case, parameters $\lambda_\alpha^{(1)} (\alpha = 1, 2, 3)$ all vanish and matrix $\mathbf{B}^{(1)}$ becomes

$$\mathbf{B}^{(1)} = \begin{bmatrix} \mathbf{B}_e^{(1)} & \mathbf{0} \\ \mathbf{0}^{\mathrm{T}} & 1 \end{bmatrix}, \tag{4.17}$$

where

$$\mathbf{B}_e^{(1)} = \begin{bmatrix} -p_1^{(1)} & -p_2^{(1)} \\ 1 & 1 \end{bmatrix},$$

is the matrix related entirely to the elastic response for the upper material. The matrices defined in Eq. (4.7) for the upper material are

$$\mathbf{L}^{(1)^{-1}} = \begin{bmatrix} Y_{11}^{(1)} & 0 & 0 \\ 0 & Y_{22}^{(1)} & 0 \\ 0 & 0 & Y_{33}^{(1)} \end{bmatrix}, \quad \mathbf{S}^{(1)}\mathbf{L}^{(1)^{-1}} = \begin{bmatrix} 0 & -\widehat{Y}_{12}^{(1)} & 0 \\ \widehat{Y}_{12}^{(1)} & 0 & 0 \\ 0 & 0 & 0 \end{bmatrix}, \tag{4.18}$$

where simplified expressions of $Y_{\alpha\alpha}^{(1)}$ ($\alpha = 1, 2, 3$, no sum on α) and $\widehat{Y}_{12}^{(1)}$ are listed in Appendix E. Matrices $\mathbf{L}^{(2)^{-1}}$ and $\mathbf{S}^{(2)}\mathbf{L}^{(2)^{-1}}$ are still given by Eq. (4.7) since the properties of the lower material are always maintained in case (A). By substituting $\mathbf{L}^{(1)^{-1}}$,$\mathbf{S}^{(1)}\mathbf{L}^{(1)^{-1}}$,$\mathbf{L}^{(2)^{-1}}$ and $\mathbf{S}^{(2)}\mathbf{L}^{(2)^{-1}}$ into Eq. (3.6), matrix $\mathbf{F}$ corresponding to *this kind of bimaterial (A–B)* can be computed. It is found that the same full matrix as that given in Eq. (4.8) is obtained, but now with different contents for the elements of $\mathbf{F}$.

(III) Bimaterial (A–C): a lower piezoelectric material jointed to an upper elastic material with $\mathbf{c}^{(1)} \neq \mathbf{0}$, $\boldsymbol{\alpha}^{(1)} = \mathbf{0}$ *and* $\mathbf{e}^{(1)} = \mathbf{0}$.

Matrix $\mathbf{F}$ corresponding to this kind of bimaterial can be obtained from the previous results for *bimaterial (A–B)* by further letting $\boldsymbol{\alpha}^{(1)} = \mathbf{0}$. The elements of $\mathbf{F}$ are as follows:

$$\begin{aligned} &F_{11} = [(Y_{11}^{(1)} - Y_{11}^{(2)})(Y_{22}^{(1)} + Y_{22}^{(2)}) - (\widehat{Y}_{12}^{(1)} - \widehat{Y}_{12}^{(2)})^2]/\widehat{F}, \quad F_{12} = -2Y_{22}^{(2)}(\widehat{Y}_{12}^{(1)} - \widehat{Y}_{12}^{(2)})/\widehat{F}, \\ &F_{21} = 2Y_{11}^{(2)}(\widehat{Y}_{12}^{(1)} - \widehat{Y}_{12}^{(2)})/\widehat{F}, \quad F_{22} = [(Y_{11}^{(1)} + Y_{11}^{(2)})(Y_{22}^{(1)} - Y_{22}^{(2)}) - (\widehat{Y}_{12}^{(1)} - \widehat{Y}_{12}^{(2)})^2]/\widehat{F}, \\ &F_{13} = -2Y_{23}^{(2)}(\widehat{Y}_{12}^{(1)} - \widehat{Y}_{12}^{(2)})/\widehat{F}, \quad F_{23} = -2Y_{23}^{(2)}(\widehat{Y}_{11}^{(1)} + \widehat{Y}_{11}^{(2)})/\widehat{F}, \quad F_{31} = F_{32} = 0, \quad F_{33} = 1, \end{aligned} \tag{4.19}$$

where $\widehat{F} = (Y_{11}^{(1)} + Y_{11}^{(2)})(Y_{22}^{(1)} + Y_{22}^{(2)}) - (\widehat{Y}_{12}^{(1)} - \widehat{Y}_{12}^{(2)})^2$ and expressions for $Y_{11}^{(1)}, Y_{22}^{(1)}$, and $\widehat{Y}_{12}^{(1)}$ are still given by Eqs. (E.1) and (E.2), as shown in Appendix E.

(IV) Bimaterial (A–D): a lower piezoelectric material jointed to an upper dielectric material with $\mathbf{c}^{(1)} = \mathbf{0}$, $\boldsymbol{\alpha}^{(1)} \neq \mathbf{0}$ *and* $\mathbf{e}^{(1)} = \mathbf{0}$.

The kernel functions corresponding to this kind of bimaterial, where the upper material is filled with a dielectric material such as air, may be obtained from *bimaterial (A–B)* by further letting $\mathbf{c}^{(1)} = \mathbf{0}$. To do this, we first express the elements of matrices $\mathbf{L}^{(1)^{-1}}$ and $\mathbf{S}^{(1)}\mathbf{L}^{(1)^{-1}}$ in Eq. (4.18) for *bimaterial (A–B)* in terms of Krenk's parameters (Krenk, 1979; Sung and Liou, 1995a), which are as follows:

$$Y_{11}^{(1)} = \frac{\sqrt{2(1+\kappa^{(1)})}}{\widehat{E}^{(1)}\delta^{(1)}}, \quad Y_{22}^{(1)} = \frac{\delta^{(1)}\sqrt{2(1+\kappa^{(1)})}}{\widehat{E}^{(1)}}, \quad Y_{33}^{(1)} = -\frac{1}{n_3^{(1)}\alpha_{22}^{(1)}}, \quad \widehat{Y}_{12}^{(1)} = \frac{(\hat{\nu}^{(1)} - 1)}{\widehat{E}^{(1)}}, \tag{4.20}$$

where $\delta^{(1)}$, $\kappa^{(1)}$, $\hat{\nu}^{(1)}$ and $\widehat{E}^{(1)}$ are Krenk's parameters for the upper material. Similarly, matrix $\mathbf{F}$ for *bimaterial (A–B)* may be reconstructed in terms of Krenk's parameters. Although the terms shown in Eq. (4.20) diverge when $\widehat{E}^{(1)} = 0$, the elements of $\mathbf{F}$ for *bimaterial (A–B)* are actually all bounded when $\widehat{E}^{(1)} = 0$. Therefore, matrix $\mathbf{F}$ for the *bimaterial (A–D)* may be obtained by letting $\widehat{E}^{(1)} = 0$ in matrix $\mathbf{F}$ for *bimaterial (A–B)*. The result is

$$\mathbf{F} = \begin{bmatrix} 1 & 0 & 0 \\ 0 & 1 & 0 \\ 0 & 2Y_{23}^{(2)}n_3^{(1)}\alpha_{22}^{(1)}/(1 - Y_{33}^{(2)}n_3^{(1)}\alpha_{22}^{(1)}) & -1 + 2/(1 - Y_{33}^{(2)}n_3^{(1)}\alpha_{22}^{(1)}) \end{bmatrix}. \tag{4.21}$$

Note that the mechanical boundary condition with $\widehat{E}^{(1)} = 0$ corresponds to the traction-free condition. Therefore, matrix $\mathbf{F}$ in Eq. (4.21) corresponds to the problem with *traction-free* and *electric-flux continuous* specified on the boundary.

Two extreme electrical boundary conditions may be considered from Eq. (4.21). First, by taking $\alpha_{22}^{(1)} = 0$ in Eq. (4.21), the electric-flux free (or simply called electric-open) condition on the boundary is obtained. For such a case, $\mathbf{F}$ becomes the identity matrix, i.e.,

$$\mathbf{F} = \begin{bmatrix} 1 & 0 & 0 \\ 0 & 1 & 0 \\ 0 & 0 & 1 \end{bmatrix}. \tag{4.22}$$

Another consideration of $\alpha_{22}^{(1)} \to \infty$ in Eq. (4.21) will lead to the electric-closed condition on the boundary, where the corresponding $\boldsymbol{F}$ is given by

$$\boldsymbol{F} = \begin{bmatrix} 1 & 0 & 0 \\ 0 & 1 & 0 \\ 0 & -2Y_{23}^{(2)}/Y_{33}^{(2)} & -1 \end{bmatrix}. \tag{4.23}$$

Comparing Eq. (4.22) with Eq. (4.23), the difference between the electric-open and electric-closed conditions is completely in the elements F_{32} and F_{33} only.

Letting $\widehat{E}^{(1)} \to \infty$ instead of letting $\widehat{E}^{(1)} = 0$ as done above, the problem of *displacement-fixed* and *electric-flux-continuous* specified on the boundary is obtained. The elements of $\boldsymbol{F}$ corresponding to this problem are as follows:

$$\begin{aligned}
F_{11} &= 1 - 2Y_{11}^{(2)}[Y_{22}^{(2)} + n_3^{(1)}\alpha_{22}^{(1)}(Y_{23}^{(2)^2} - Y_{22}^{(2)}Y_{33}^{(2)})]/\widehat{F},\\
F_{12} &= 2\widehat{Y}_{12}^{(2)}[Y_{22}^{(2)} + n_3^{(1)}\alpha_{22}^{(1)}(Y_{23}^{(2)^2} - Y_{22}^{(2)}Y_{33}^{(2)})]/\widehat{F},\\
F_{13} &= 2[Y_{23}^{(2)}\widehat{Y}_{12}^{(2)} + n_3^{(1)}\alpha_{22}^{(1)}\widehat{Y}_{13}^{(2)}(Y_{23}^{(2)^2} - Y_{22}^{(2)}Y_{33}^{(2)})]/\widehat{F},\\
F_{21} &= 2Y_{11}^{(2)}[\widehat{Y}_{12}^{(2)}(n_3^{(1)}\alpha_{22}^{(1)}Y_{33}^{(2)} - 1) - n_3^{(1)}\alpha_{22}^{(1)}Y_{23}^{(2)}\widehat{Y}_{13}^{(2)}]/\widehat{F},\\
F_{22} &= -1 + 2\widehat{Y}_{12}^{(2)}[\widehat{Y}_{12}^{(2)}(n_3^{(1)}\alpha_{22}^{(1)}Y_{33}^{(2)} - 1) - n_3^{(1)}\alpha_{22}^{(1)}Y_{23}^{(2)}\widehat{Y}_{13}^{(2)}]/\widehat{F},\\
F_{23} &= -2[Y_{11}^{(2)}Y_{23}^{(2)} + n_3^{(1)}\alpha_{22}^{(1)}\widehat{Y}_{13}^{(2)}(Y_{23}^{(2)}\widehat{Y}_{13}^{(2)} - Y_{33}^{(2)}\widehat{Y}_{12}^{(2)})]/\widehat{F},\\
F_{31} &= -2n_3^{(1)}\alpha_{22}^{(1)}Y_{11}^{(2)}(Y_{23}^{(2)}\widehat{Y}_{12}^{(2)} - Y_{22}^{(2)}\widehat{Y}_{13}^{(2)})/\widehat{F},\\
F_{32} &= -2n_3^{(1)}\alpha_{22}^{(1)}\widehat{Y}_{12}^{(2)}(Y_{23}^{(2)}\widehat{Y}_{12}^{(2)} - Y_{22}^{(2)}\widehat{Y}_{13}^{(2)})/\widehat{F},\\
F_{33} &= \{Y_{11}^{(2)}[Y_{22}^{(2)}(1 + n_3^{(1)}\alpha_{22}^{(1)}Y_{33}^{(2)}) - n_3^{(1)}\alpha_{22}^{(1)}Y_{23}^{(2)^2}] - \widehat{Y}_{12}^{(2)^2}(1 + n_3^{(1)}\alpha_{22}^{(1)}Y_{33}^{(2)}) + n_3^{(1)}\alpha_{22}^{(1)}Y_{22}^{(2)}\widehat{Y}_{13}^{(2)^2}\}/\widehat{F},
\end{aligned} \tag{4.24}$$

where

$$\widehat{F} = \left\{Y_{11}^{(2)}[Y_{22}^{(2)} + n_3^{(1)}\alpha_{22}^{(1)}(Y_{23}^{(2)^2} - Y_{22}^{(2)}Y_{33}^{(2)})] + \widehat{Y}_{12}^{(2)^2}(n_3^{(1)}\alpha_{22}^{(1)}Y_{33}^{(2)} - 1) + n_3^{(1)}\alpha_{22}^{(1)}\widehat{Y}_{13}^{(2)}[Y_{22}^{(2)}\widehat{Y}_{13}^{(2)} - 2Y_{23}^{(2)}\widehat{Y}_{12}^{(2)}]\right\}.$$

Two extreme electrical boundary conditions may also be considered from Eq. (4.24). One is taking $\alpha_{22}^{(1)} = 0$ in the above equation. We get matrix $\boldsymbol{F}$ for the problem with *displacement-fixed* and *electric-flux free* on the boundary where elements of $\boldsymbol{F}$ are

$$\begin{aligned}
&F_{11} = 1 + 2Y_{11}^{(2)}Y_{22}^{(2)}/(\widehat{Y}_{12}^{(2)^2} - Y_{11}^{(2)}Y_{22}^{(2)}), \quad F_{12} = -2Y_{22}^{(2)}\widehat{Y}_{12}^{(2)}/(\widehat{Y}_{12}^{(2)^2} - Y_{11}^{(2)}Y_{22}^{(2)}),\\
&F_{13} = -2Y_{23}^{(2)}\widehat{Y}_{12}^{(2)}/(\widehat{Y}_{12}^{(2)^2} - Y_{11}^{(2)}Y_{22}^{(2)}), \quad F_{21} = 2Y_{11}^{(2)}\widehat{Y}_{12}^{(2)}/(\widehat{Y}_{12}^{(2)^2} - Y_{11}^{(2)}Y_{22}^{(2)}),\\
&F_{22} = -1 + 2\widehat{Y}_{12}^{(2)^2}/(\widehat{Y}_{12}^{(2)^2} - Y_{11}^{(2)}Y_{22}^{(2)}), \quad F_{23} = 2Y_{11}^{(2)}Y_{23}^{(2)}/(\widehat{Y}_{12}^{(2)^2} - Y_{11}^{(2)}Y_{22}^{(2)}),\\
&F_{31} = F_{32} = 0, \quad F_{33} = 1.
\end{aligned} \tag{4.25}$$

The other is taking $\alpha_{22}^{(1)} \to \infty$ in Eq. (4.24). The *displacement-fixed* and *electric-closed* problem is obtained with the elements of $\boldsymbol{F}$ given as

$$\begin{aligned}
&F_{11} = 1 - 2Y_{11}^{(2)}(Y_{23}^{(2)^2} - Y_{22}^{(2)}Y_{33}^{(2)})/\widehat{F}, \quad F_{12} = 2\widehat{Y}_{12}^{(2)}(Y_{23}^{(2)^2} - Y_{22}^{(2)}Y_{33}^{(2)})/\widehat{F},\\
&F_{13} = 2\widehat{Y}_{13}^{(2)}(Y_{23}^{(2)^2} - Y_{22}^{(2)}Y_{33}^{(2)})/\widehat{F}, \quad F_{21} = 2Y_{11}^{(2)}(Y_{33}^{(2)}\widehat{Y}_{12}^{(2)} - Y_{23}^{(2)}\widehat{Y}_{13}^{(2)})/\widehat{F},\\
&F_{22} = -1 + 2\widehat{Y}_{12}^{(2)}(Y_{33}^{(2)}\widehat{Y}_{12}^{(2)} - Y_{23}^{(2)}\widehat{Y}_{13}^{(2)})/\widehat{F}, \quad F_{23} = -2\widehat{Y}_{13}^{(2)}(Y_{23}^{(2)}\widehat{Y}_{13}^{(2)} - Y_{33}^{(2)}\widehat{Y}_{12}^{(2)})/\widehat{F},\\
&F_{31} = -2Y_{11}^{(2)}(Y_{23}^{(2)}\widehat{Y}_{12}^{(2)} - Y_{22}^{(2)}\widehat{Y}_{13}^{(2)})/\widehat{F}, \quad F_{32} = -2\widehat{Y}_{12}^{(2)}(Y_{23}^{(2)}\widehat{Y}_{12}^{(2)} - Y_{22}^{(2)}\widehat{Y}_{13}^{(2)})/\widehat{F},\\
&F_{33} = [Y_{11}^{(2)}(Y_{22}^{(2)}Y_{33}^{(2)} - Y_{23}^{(2)^2}) - Y_{33}^{(2)}\widehat{Y}_{12}^{(2)^2} + Y_{22}^{(2)}\widehat{Y}_{13}^{(2)^2}]/\widehat{F},
\end{aligned} \tag{4.26}$$

where

$$\widehat{F} = [Y_{11}^{(2)}(Y_{23}^{(2)^2} - Y_{22}^{(2)}Y_{33}^{(2)}) + Y_{33}^{(2)}\widehat{Y}_{12}^{(2)^2} + \widehat{Y}_{13}^{(2)}(Y_{22}^{(2)}\widehat{Y}_{13}^{(2)} - 2Y_{23}^{(2)}\widehat{Y}_{12}^{(2)})].$$

(V) Bimaterial (A–E): a lower piezoelectric material jointed to an upper vacuum with $\boldsymbol{c}^{(1)} = \boldsymbol{0}$, $\boldsymbol{\alpha}^{(1)} = \boldsymbol{0}$ *and* $\boldsymbol{e}^{(1)} = \boldsymbol{0}$ (*half-plane problem*)

This case is exactly the same as that discussed in Eq. (4.22), i.e., *bimaterial (A–E)* which corresponds to the half-plane problem with *traction-free* and *electric-flux free* conditions specified on the boundary, where matrix $\boldsymbol{F}$ is a 3×3 unit matrix. Note that the kernel functions corresponding to *bimaterial (A–E)* have been addressed by Yang et al. (2007).

4.2. Kernel functions for special lower materials

In the previous subsection, all the discussions are based on the assumption that the condition $\boldsymbol{c}^{(2)} \neq \boldsymbol{0}$, $\boldsymbol{\alpha}^{(2)} \neq \boldsymbol{0}$ and $\boldsymbol{e}^{(2)} \neq \boldsymbol{0}$, classified as case A, always holds for the lower half-plane material. Similar to the discussions made above, we may develop the special kernel functions if the lower material belongs to other cases, i.e., when the lower material varies from case B to case E. We will not repeat all the discussions for all possible cases for the bimaterials. Instead, we consider the case when the lower and upper materials both belong to case B, i.e., we further discuss the kernel functions corresponding to the *bimaterial (B–B)*, which is the bimaterial composed by an *elastic-electric decoupled* material jointed to another *elastic-electric decoupled* material. Since the mechanical and electric coupling effect vanishes for both upper and lower materials, the original coupled problem is reduced to two separate purely anisotropic elastic bimaterial and purely electric bimaterial problems. The kernel functions for this *bimaterial (B–B)* may be obtained from the *bimaterial (A–B)* discussed above by further letting $\boldsymbol{e}^{(2)} = \boldsymbol{0}$ for the lower material. Note that the condition of the piezoelectric-stress constants $\boldsymbol{e}^{(2)} = \boldsymbol{0}$ for the lower material implies that matrix $\boldsymbol{B}^{(2)}$ defined in Eq. (4.6) takes the same form as that in Eq. (4.17) for the upper material since parameters $\lambda_\alpha^{(2)}(\alpha = 1,2,3)$ defined in Appendix A all vanish when $\boldsymbol{e}^{(2)} = \boldsymbol{0}$. With the vanishing of both parameters $\lambda_\alpha^{(1)}$ and $\lambda_\alpha^{(2)}(\alpha = 1,2,3)$, expressions of $Y_{23}^{(j)}$ and $\widehat{Y}_{13}^{(j)}(j = 1,2)$ defined in Appendix B also vanish. With these observations, the elements of matrix $\boldsymbol{F}$ for *bimaterial (B–B)*can be written as

$$
\begin{aligned}
&F_{11} = \frac{(Y_{11}^{(1)} - Y_{11}^{(2)})(Y_{22}^{(1)} + Y_{22}^{(2)}) - (\widehat{Y}_{12}^{(1)} - \widehat{Y}_{12}^{(2)})^2}{(Y_{11}^{(1)} + Y_{11}^{(2)})(Y_{22}^{(1)} + Y_{22}^{(2)}) - (\widehat{Y}_{12}^{(1)} - \widehat{Y}_{12}^{(2)})^2}, \quad F_{12} = \frac{-2Y_{22}^{(2)}(\widehat{Y}_{12}^{(1)} - \widehat{Y}_{12}^{(2)})}{(Y_{11}^{(1)} + Y_{11}^{(2)})(Y_{22}^{(1)} + Y_{22}^{(2)}) - (\widehat{Y}_{12}^{(1)} - \widehat{Y}_{12}^{(2)})^2}, \\
&F_{21} = \frac{2Y_{11}^{(2)}(\widehat{Y}_{12}^{(1)} - \widehat{Y}_{12}^{(2)})}{(Y_{11}^{(1)} + Y_{11}^{(2)})(Y_{22}^{(1)} + Y_{22}^{(2)}) - (\widehat{Y}_{12}^{(1)} - \widehat{Y}_{12}^{(2)})^2}, \quad F_{22} = \frac{(Y_{11}^{(1)} + Y_{11}^{(2)})(Y_{22}^{(1)} - Y_{22}^{(2)}) - (\widehat{Y}_{12}^{(1)} - \widehat{Y}_{12}^{(2)})^2}{(Y_{11}^{(1)} + Y_{11}^{(2)})(Y_{22}^{(1)} + Y_{22}^{(2)}) - (\widehat{Y}_{12}^{(1)} - \widehat{Y}_{12}^{(2)})^2}, \\
&F_{33} = -1 + \frac{2Y_{33}^{(1)}}{Y_{33}^{(1)} + Y_{33}^{(2)}}, \quad F_{13} = F_{23} = F_{31} = F_{32} = 0,
\end{aligned}
\tag{4.27}
$$

where $Y_{11}^{(j)}, Y_{22}^{(j)}, Y_{33}^{(j)}$, and $\widehat{Y}_{12}^{(j)}(j = 1,2)$ are listed in Appendix E. It can be shown that the elastic part of matrix $\boldsymbol{F}$ in Eq. (4.27), i.e., F_{11}, F_{12}, F_{21}, and F_{22}, exactly reproduce the 2×2 matrix $\boldsymbol{M}$ defined in the paper by Sung and Liou (1995b), if the following relationships:

$$
\begin{aligned}
n_1^{(j)} &= \delta^{(j)}[(\frac{\kappa^{(j)} + 1}{2})^{1/2} + (\frac{\kappa^{(j)} - 1}{2})^{1/2}], \\
n_2^{(j)} &= \delta^{(j)}[(\frac{\kappa^{(j)} + 1}{2})^{1/2} - (\frac{\kappa^{(j)} - 1}{2})^{1/2}], \quad (j = 1,2),
\end{aligned}
\tag{4.28}
$$

for type I roots and

$$
m_1^{(j)} = \delta^{(j)}(\frac{1 - \kappa^{(j)}}{2})^{1/2}, \quad n_1^{(j)} = \delta^{(j)}(\frac{1 + \kappa^{(j)}}{2})^{1/2}, \quad (j = 1,2),
\tag{4.29}
$$

for type II roots and

$$
c_{11}^{(j)} = \frac{\delta^{(j)^2}\widehat{E}^{(j)}}{1 - \hat{\nu}^{(j)^2}}, \quad c_{22}^{(j)} = \frac{\widehat{E}^{(j)}}{\delta^{(j)^2}(1 - \hat{\nu}^{(j)^2})}, \quad c_{12}^{(j)} = \frac{\hat{\nu}^{(j)}\widehat{E}^{(j)}}{1 - \hat{\nu}^{(j)^2}}, \quad c_{44}^{(j)} = \frac{\widehat{E}^{(j)}}{2(\kappa^{(j)} + \hat{\nu}^{(j)})},
\tag{4.30}
$$

are used. Note that element F_{33} in Eq. (4.27) is the term related to the purely electric bimaterial response which is not available from purely elastic bimaterial analysis, as made earlier by Sung and Liou (1995b). Now with matrix $\boldsymbol{B}^{(j)}(j = 1, 2)$ both expressed in the form as in Eq. (4.17) and with matrix $\boldsymbol{F}$ discussed above, the kernel functions for the mechanical and electric decoupled problem become

$$
\boldsymbol{K}(\xi, t) = \frac{1}{\widehat{B}_i^{(2)^2}} \begin{bmatrix} K_i^{11} & K_i^{12} & 0 \\ K_i^{21} & K_i^{22} & 0 \\ 0 & 0 & K_i^{33} \end{bmatrix}.
\tag{4.31}
$$

Although detailed expressions of the elements of $\boldsymbol{K}(\xi, t)$ are not given here, it can be shown that, with some algebraic manipulations, the elastic part of the kernel functions in Eq. (4.31), for both type I and type II roots (i = I, II), do indeed recover those presented by Sung and Liou (1995b). The present analyses, however, have the benefits that the kernel functions corresponding to the *purely electric bimaterial* problems are produced simultaneously without extra effort. Note that the kernel functions for the degenerated *isotropic bimaterial* problems are embedded in the results given in Eq. (4.31). The part corresponding to the *elastic isotropic bimaterial* has been addressed by Sung and Liou (1995b). Here, we give the kernel functions for the part of the *electric isotropic biomaterial*, which is

$$
K_{\mathrm{I}}^{33} = K_{\mathrm{II}}^{33} = \frac{(\alpha_{22}^{(2)} - \alpha_{22}^{(1)})(\xi - t)}{(\alpha_{22}^{(1)} + \alpha_{22}^{(2)})[4d^2 + (\xi - t)^2]}.
\tag{4.32}
$$

5. Results and discussions

In the previous section, it has been shown that by considering certain properties of the upper material, the kernel functions for a horizontal crack embedded in a lower half-plane piezoelectric solid can be obtained. The mechanical boundary conditions on the half-plane boundary may be either traction-free or displacement-fixed. The electric boundary conditions specified on the boundary may be *electrical-flux continuous* (*e.g. take air as the upper material*), *electrical-open*, or *electric-*

Table 1
Normalized generalized stress intensity factors for the half-plane *traction-free* problem with various electric boundary conditions subjected to uniform pressure loading ($\boldsymbol{\alpha}^{(1)} = \boldsymbol{\alpha}_{\mathrm{Air}}$: electric-flux continuous, $\boldsymbol{\alpha}^{(1)} \to \infty$: electric-closed, $\boldsymbol{\alpha}^{(1)} = \boldsymbol{0}$: electric-open)

SIF	$\boldsymbol{\alpha}^{(1)}$	d/c					
		0.1	0.2	0.4	1.0	2.0	4.0
k_{I}^{*}	$\boldsymbol{\alpha}^{(1)} = \boldsymbol{\alpha}_{\mathrm{Air}}$	12.7304	5.5615	2.8148	1.5248	1.1833	1.0543
	$\boldsymbol{\alpha}^{(1)} \to \infty$	12.7560	5.5845	2.8320	1.5331	1.1867	1.0554
	$\boldsymbol{\alpha}^{(1)} = \boldsymbol{0}$	12.7301	5.5613	2.8147	1.5248	1.1833	1.0543
	(Purely elastic)	(12.7220)	(5.5760)	(2.8325)	(1.5381)	(1.1913)	(1.0576)
k_{II}^{*}	$\boldsymbol{\alpha}^{(1)} = \boldsymbol{\alpha}_{\mathrm{Air}}$	−7.8169	−2.7000	−0.8949	−0.1757	−0.0391	−0.0064
	$\boldsymbol{\alpha}^{(1)} \to \infty$	−7.8226	−2.7020	−0.8957	−0.1764	−0.0394	−0.0065
	$\boldsymbol{\alpha}^{(1)} = \boldsymbol{0}$	−7.8168	−2.7000	−0.8949	−0.1757	−0.0391	−0.0064
	(Purely elastic)	(−7.7787)	(−2.6909)	(−0.8953)	(−0.1784)	(−0.0406)	(−0.0069)
k_{D}^{*}	$\boldsymbol{\alpha}^{(1)} = \boldsymbol{\alpha}_{\mathrm{Air}}$	8.4683	3.0095	1.0671	0.2626	0.083	0.0233
	$\boldsymbol{\alpha}^{(1)} \to \infty$	8.9759	3.5858	1.4746	0.4202	0.1352	0.0375
	$\boldsymbol{\alpha}^{(1)} = \boldsymbol{0}$	8.4566	3.0050	1.0654	0.2622	0.0829	0.0233
	(Purely electric)	(No such data)					

Table 2
Normalized generalized stress intensity factors for the half-plane *traction-free* problem with various electric boundary conditions subjected to uniform shear loading ($\boldsymbol{\alpha}^{(1)} = \boldsymbol{\alpha}_{\mathrm{Air}}$: electric-flux continuous, $\boldsymbol{\alpha}^{(1)} \to \infty$: electric-closed, $\boldsymbol{\alpha}^{(1)} = \boldsymbol{0}$: electric-open)

SIF	$\boldsymbol{\alpha}^{(1)}$	d/c					
		0.1	0.2	0.4	1.0	2.0	4.0
k_{I}^{*}	$\boldsymbol{\alpha}^{(1)} = \boldsymbol{\alpha}_{\mathrm{Air}}$	0.7758	0.5467	0.3414	0.1210	0.0341	0.0062
	$\boldsymbol{\alpha}^{(1)} \to \infty$	0.7760	0.5466	0.3411	0.1212	0.0343	0.0063
	$\boldsymbol{\alpha}^{(1)} = \boldsymbol{0}$	0.7758	0.5467	0.3414	0.1210	0.0341	0.0062
	(Purely elastic)	(0.7735)	(0.5450)	(0.3400)	(0.1210)	(0.0346)	(0.0064)
k_{II}^{*}	$\boldsymbol{\alpha}^{(1)} = \boldsymbol{\alpha}_{\mathrm{Air}}$	1.2909	1.1494	1.0940	1.0608	1.0311	1.0108
	$\boldsymbol{\alpha}^{(1)} \to \infty$	1.2924	1.1510	1.0954	1.0614	1.0313	1.0109
	$\boldsymbol{\alpha}^{(1)} = \boldsymbol{0}$	1.2909	1.1494	1.0940	1.0608	1.0311	1.0108
	(Purely elastic)	(1.2865)	(1.1468)	(1.0922)	(1.0592)	(1.0303)	(1.0106)
k_{D}^{*}	$\boldsymbol{\alpha}^{(1)} = \boldsymbol{\alpha}_{\mathrm{Air}}$	0.5756	0.3956	0.2337	0.0705	0.0171	0.0029
	$\boldsymbol{\alpha}^{(1)} \to \infty$	0.4306	0.3035	0.1868	0.0625	0.0163	0.0028
	$\boldsymbol{\alpha}^{(1)} = \boldsymbol{0}$	0.5762	0.3959	0.2338	0.0706	0.0171	0.0029
	(Purely electric)	(No such data)					

Table 3
Normalized generalized stress intensity factors for the half-plane *traction-free* problem with various electric boundary conditions subjected to uniform electric displacement loading ($\boldsymbol{\alpha}^{(1)} = \boldsymbol{\alpha}_{\mathrm{Air}}$: electric-flux continuous, $\boldsymbol{\alpha}^{(1)} \to \infty$: electric-closed, $\boldsymbol{\alpha}^{(1)} = \boldsymbol{0}$: electric-open)

SIF	$\boldsymbol{\alpha}^{(1)}$	d/c					
		0.1	0.2	0.4	1.0	2.0	4.0
k_{I}^{*}	$\boldsymbol{\alpha}^{(1)} = \boldsymbol{\alpha}_{\mathrm{Air}}$	0.0253	0.0191	0.0141	0.0084	0.0043	0.0015
	$\boldsymbol{\alpha}^{(1)} \to \infty$	−0.0027	−0.0016	0.0001	0.0024	0.0022	0.0010
	$\boldsymbol{\alpha}^{(1)} = \boldsymbol{0}$	0.0256	0.0192	0.0142	0.0084	0.0043	0.0015
	(Purely elastic)	(No such data)					
k_{II}^{*}	$\boldsymbol{\alpha}^{(1)} = \boldsymbol{\alpha}_{\mathrm{Air}}$	−0.0103	−0.0079	−0.006	−0.0033	−0.0012	−0.0002
	$\boldsymbol{\alpha}^{(1)} \to \infty$	−0.0086	−0.0077	−0.0062	−0.0033	−0.0012	−0.0002
	$\boldsymbol{\alpha}^{(1)} = \boldsymbol{0}$	−0.0103	−0.0079	−0.0060	−0.0033	−0.0012	−0.0002
	(Purely elastic)	(No such data)					
k_{D}^{*}	$\boldsymbol{\alpha}^{(1)} = \boldsymbol{\alpha}_{\mathrm{Air}}$	1.9999	1.5651	1.2845	1.0862	1.0270	1.0073
	(Purely electric)	(2.0168)	(1.5752)	(1.2894)	(1.0868)	(1.0267)	(1.0072)
	$\boldsymbol{\alpha}^{(1)} \to \infty$	0.7547	0.7883	0.8407	0.9319	0.9772	0.9938
	(Purely electric)	(0.7547)	(0.7868)	(0.8370)	(0.9271)	(0.9746)	(0.9929)
	$\boldsymbol{\alpha}^{(1)} = \boldsymbol{0}$	2.0124	1.5697	1.2862	1.0866	1.0271	1.0074
	(Purely electric)	(2.0320)	(1.5809)	(1.2915)	(1.0873)	(1.0269)	(1.0072)

closed. Therefore, to see the effect of the electric boundary conditions, the developed kernel functions are used to investigate half-plane problems with either the mechanical traction-free condition or mechanical displacement-fixed condition. The bimaterial subinterface crack problems are then analyzed where the kernel functions in equations Eq. (3.11) are used. Combined with the auxiliary condition specified in Eq. (3.14), the system of singular integral equations is solved numerically for all problems discussed below using a method suggested by Gerasoulis (1982). This method uses piecewise quadratic poly-

Table 4
Normalized generalized stress intensity factors for the half-plane *displacement-fixed* problem with various electric boundary conditions subjected to uniform pressure loading ($\boldsymbol{\alpha}^{(1)} = \boldsymbol{\alpha}_{Air}$: electric-flux continuous, $\boldsymbol{\alpha}^{(1)} \to \infty$: electric-closed, $\boldsymbol{\alpha}^{(1)} = \boldsymbol{0}$: electric-open)

SIF	$\boldsymbol{\alpha}^{(1)}$	d/c					
		0.1	0.2	0.4	1.0	2.0	4.0
k_I^*	$\boldsymbol{\alpha}^{(1)} = \boldsymbol{\alpha}_{Air}$	0.6823	0.7103	0.7460	0.8172	0.8986	0.9631
	$\boldsymbol{\alpha}^{(1)} \to \infty$	0.6935	0.7187	0.7524	0.8218	0.9011	0.964
	$\boldsymbol{\alpha}^{(1)} = \boldsymbol{0}$	0.6823	0.7102	0.7460	0.8172	0.8986	0.9631
	(Purely elastic)	(0.6967)	(0.7196)	(0.7509)	(0.8171)	(0.8953)	(0.9608)
k_{II}^*	$\boldsymbol{\alpha}^{(1)} = \boldsymbol{\alpha}_{Air}$	0.1933	0.1543	0.1164	0.0619	0.0221	0.0044
	$\boldsymbol{\alpha}^{(1)} \to \infty$	0.1893	0.1502	0.1126	0.0597	0.0214	0.0043
	$\boldsymbol{\alpha}^{(1)} = \boldsymbol{0}$	0.1933	0.1543	0.1164	0.0619	0.0221	0.0044
	(Purely elastic)	(0.1719)	(0.1387)	(0.1068)	(0.0592)	(0.0223)	(0.0047)
k_D^*	$\boldsymbol{\alpha}^{(1)} = \boldsymbol{\alpha}_{Air}$	0.0164	0.0064	−0.0038	−0.0147	−0.0125	−0.0053
	$\boldsymbol{\alpha}^{(1)} \to \infty$	−0.0667	−0.0547	−0.0496	−0.0454	−0.0276	−0.0102
	$\boldsymbol{\alpha}^{(1)} = \boldsymbol{0}$	0.0170	0.0067	−0.0036	−0.0146	−0.0125	−0.0052
	(Purely electric)	(No such data)					

Table 5
Normalized generalized stress intensity factors for the half-plane *displacement-fixed* problem with various electric boundary conditions subjected to uniform shear loading ($\boldsymbol{\alpha}^{(1)} = \boldsymbol{\alpha}_{Air}$: electric-flux continuous, $\boldsymbol{\alpha}^{(1)} \to \infty$: electric-closed, $\boldsymbol{\alpha}^{(1)} = \boldsymbol{0}$: electric-open)

SIF	$\boldsymbol{\alpha}^{(1)}$	d/c					
		0.1	0.2	0.4	1.0	2.0	4.0
k_I^*	$\boldsymbol{\alpha}^{(1)} = \boldsymbol{\alpha}_{Air}$	−0.2353	−0.1945	−0.1495	−0.0757	−0.0251	−0.0048
	$\boldsymbol{\alpha}^{(1)} \to \infty$	−0.1832	−0.1546	−0.1246	−0.0678	−0.0232	−0.0045
	$\boldsymbol{\alpha}^{(1)} = \boldsymbol{0}$	−0.2356	−0.1947	−0.1496	−0.0757	−0.0251	−0.0048
	(Purely elastic)	(−0.1829)	(−0.1536)	(−0.1231)	(−0.0675)	(−0.0239)	(−0.0047)
k_{II}^*	$\boldsymbol{\alpha}^{(1)} = \boldsymbol{\alpha}_{Air}$	0.7335	0.7897	0.8585	0.9309	0.9673	0.9889
	$\boldsymbol{\alpha}^{(1)} \to \infty$	0.7623	0.8178	0.8854	0.9461	0.9733	0.9907
	$\boldsymbol{\alpha}^{(1)} = \boldsymbol{0}$	0.7335	0.7896	0.8584	0.9309	0.9673	0.9889
	(Purely elastic)	(0.7514)	(0.8091)	(0.8794)	(0.9450)	(0.9733)	(0.9907)
k_D^*	$\boldsymbol{\alpha}^{(1)} = \boldsymbol{\alpha}_{Air}$	0.1558	0.1269	0.0738	0.0107	−0.0003	−0.0003
	$\boldsymbol{\alpha}^{(1)} \to \infty$	−0.3140	−0.2262	−0.1363	−0.0436	−0.0112	−0.0019
	$\boldsymbol{\alpha}^{(1)} = \boldsymbol{0}$	0.1578	0.1281	0.0744	0.0108	−0.0003	−0.0003
	(Purely electric)	(No such data)					

Table 6
Normalized generalized stress intensity factors for the half-plane *displacement-fixed* problem with various electric boundary conditions subjected to uniform electric displacement loading ($\boldsymbol{\alpha}^{(1)} = \boldsymbol{\alpha}_{Air}$: electric-flux continuous, $\boldsymbol{\alpha}^{(1)} \to \infty$: electric-closed, $\boldsymbol{\alpha}^{(1)} = \boldsymbol{0}$: electric-open)

SIF	$\boldsymbol{\alpha}^{(1)}$	d/c					
		0.1	0.2	0.4	1.0	2.0	4.0
k_I^*	$\boldsymbol{\alpha}^{(1)} = \boldsymbol{\alpha}_{Air}$	−0.1501	−0.0965	−0.0588	−0.0266	−0.0117	−0.0039
	$\boldsymbol{\alpha}^{(1)} \to \infty$	0.0057	0.0023	−0.0012	−0.0045	−0.0037	−0.0016
	$\boldsymbol{\alpha}^{(1)} = \boldsymbol{0}$	−0.1517	−0.0972	−0.0591	−0.0267	−0.0117	−0.0039
	(Purely elastic)	(No such data)					
k_{II}^*	$\boldsymbol{\alpha}^{(1)} = \boldsymbol{\alpha}_{Air}$	0.0812	0.0532	0.0292	0.0088	0.0024	0.0004
	$\boldsymbol{\alpha}^{(1)} \to \infty$	−0.0252	−0.0159	−0.0067	0.0003	0.0007	0.0002
	$\boldsymbol{\alpha}^{(1)} = \boldsymbol{0}$	0.0824	0.0537	0.0293	0.0088	0.0024	0.0004
	(Purely elastic)	(No such data)					
k_D^*	$\boldsymbol{\alpha}^{(1)} = \boldsymbol{\alpha}_{Air}$	1.9419	1.5297	1.2661	1.0795	1.0240	1.0063
	(Purely electric)	(2.0168)	(1.5752)	(1.2894)	(1.0868)	(1.0267)	(1.0072)
	$\boldsymbol{\alpha}^{(1)} \to \infty$	0.7688	0.7969	0.8436	0.9288	0.9745	0.9927
	(Purely electric)	(0.7547)	(0.7868)	(0.8370)	(0.9271)	(0.9746)	(0.9929)
	$\boldsymbol{\alpha}^{(1)} = \boldsymbol{0}$	1.9543	1.5345	1.2679	1.0800	1.0241	1.0063
	(Purely electric)	(2.0320)	(1.5809)	(1.2915)	(1.0873)	(1.0269)	(1.0072)

nomials to approximate the continuous functions $\boldsymbol{v}^{*}(t)$ ($\boldsymbol{v}^{*}(t) = \sqrt{c^2 - t^2}\boldsymbol{v}(t)$). The generalized stress intensity factors at the tips of the crack are then obtained from Eq. (3.15). The numerical procedures of Gerasoulis are described in the paper by Sung and Liou (1995c). Readers interested in the detailed numerical procedures may refer to that paper.

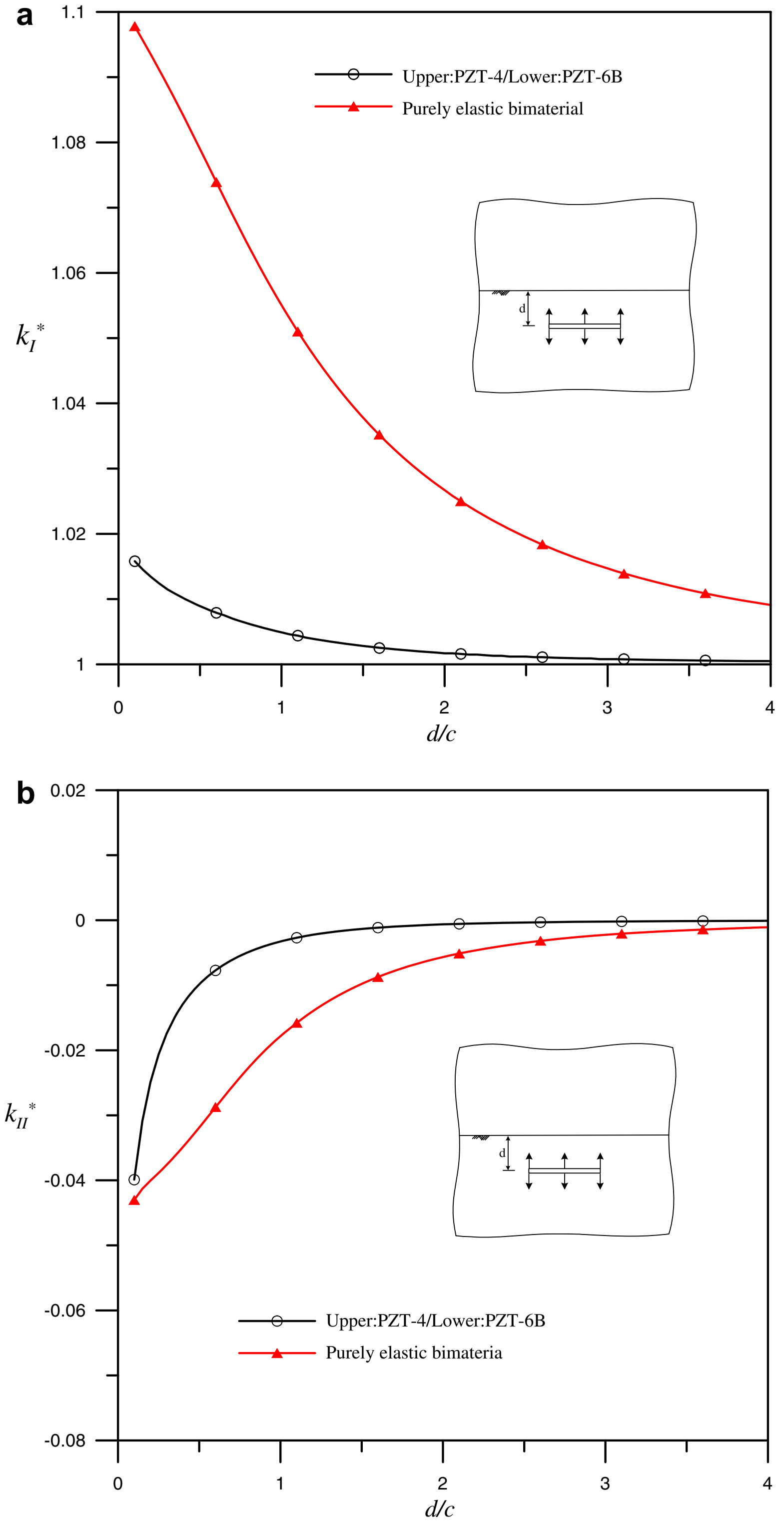

Fig. 2. Normalized generalized stress intensity factor (a) k_{I}^{*}, (b) k_{II}^{*} and (c) k_{D}^{*} for a piezoelectric bimaterial subjected to uniform pressure loading. The responses for the purely elastic bimaterial are also plotted.

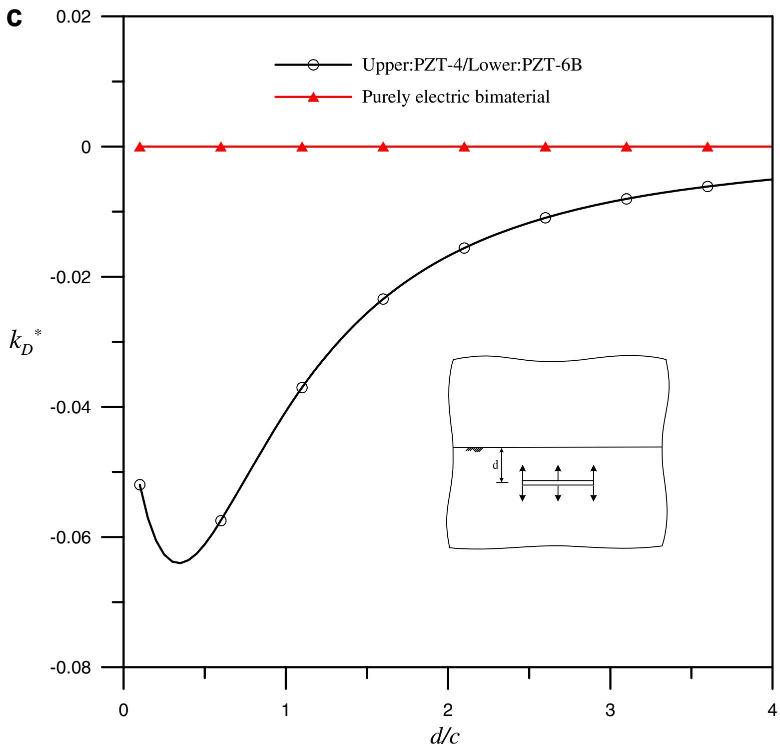

Fig. 2 (*continued*)

In the following presentations, the non-dimensional generalized stress intensity factors $[k_{\mathrm{II}}^*, k_{\mathrm{I}}^*, k_{\mathrm{D}}^*] = [k_{\mathrm{II}}/\tau, k_{\mathrm{I}}/\sigma, k_{\mathrm{D}}/D]/\sqrt{\pi c}$ are used. Here σ, τ, and D denote the magnitude of the applied uniform pressure, uniform in-plane shear, and normal electric displacement on the crack faces, respectively. Two piezoelectric materials are considered in this study. The first is PZT-6B (of type I) and the second is PZT-4 (of type II). The constants for these materials are listed below.

(1) PZT-6B

$$\boldsymbol{C} = \begin{bmatrix} 16.80 & 6.00 & 6.00 & 0 & 0 & 0 \\ 6.00 & 16.30 & 6.00 & 0 & 0 & 0 \\ 6.00 & 6.00 & 16.80 & 0 & 0 & 0 \\ 0 & 0 & 0 & 2.71 & 0 & 0 \\ 0 & 0 & 0 & 0 & 5.40 & 0 \\ 0 & 0 & 0 & 0 & 0 & 2.71 \end{bmatrix} (10^{10}\ \mathrm{Nm}^{-2}),$$

$$\boldsymbol{e}^{\mathrm{T}} = \begin{bmatrix} 0 & 0 & 0 & 0 & 0 & 4.6 \\ -0.9 & 7.1 & -0.9 & 0 & 0 & 0 \\ 0 & 0 & 0 & 4.6 & 0 & 0 \end{bmatrix} (\mathrm{Cm}^{-2}),$$

$$\boldsymbol{\alpha} = \begin{bmatrix} 36 & 0 & 0 \\ 0 & 34 & 0 \\ 0 & 0 & 36 \end{bmatrix} (10^{-10}\ \mathrm{CV}^{-1}\ \mathrm{m}^{-1}).$$

(2) PZT-4

$$\boldsymbol{C} = \begin{bmatrix} 13.90 & 7.43 & 7.78 & 0 & 0 & 0 \\ 7.43 & 11.30 & 7.43 & 0 & 0 & 0 \\ 7.78 & 7.43 & 13.90 & 0 & 0 & 0 \\ 0 & 0 & 0 & 2.56 & 0 & 0 \\ 0 & 0 & 0 & 0 & 3.06 & 0 \\ 0 & 0 & 0 & 0 & 0 & 2.56 \end{bmatrix} (10^{10}\ \mathrm{Nm}^{-2}),$$

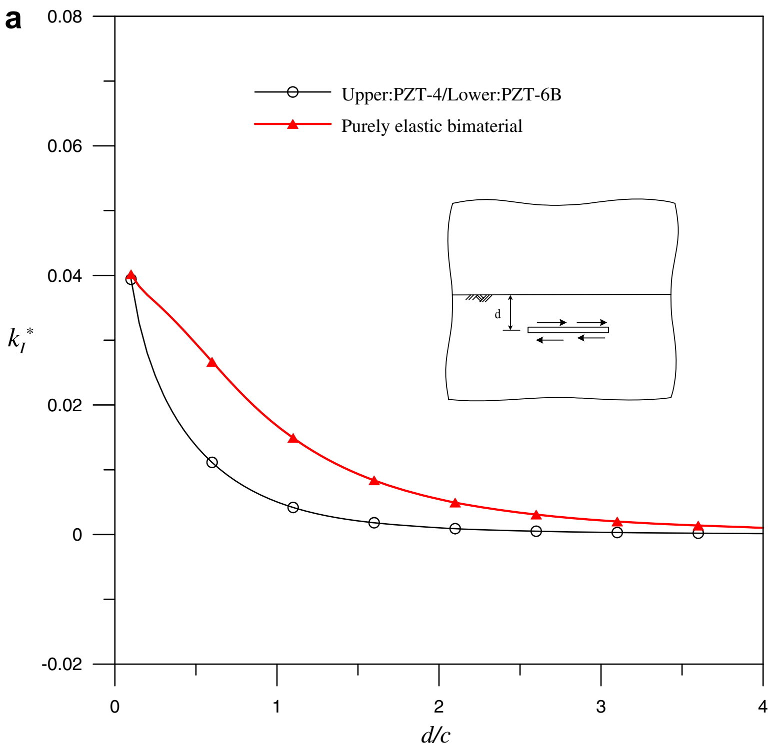

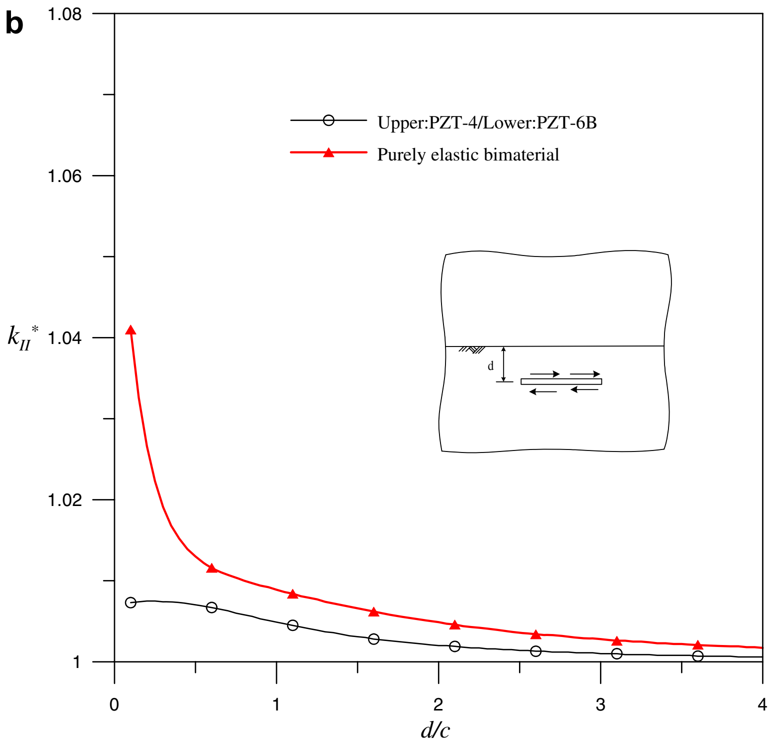

Fig. 3. Normalized generalized stress intensity factor (a) k_{I}^*, (b) k_{II}^* and (c) k_{D}^* for a piezoelectric bimaterial subjected to uniform shear loading. The responses for the purely elastic bimaterial are also plotted.

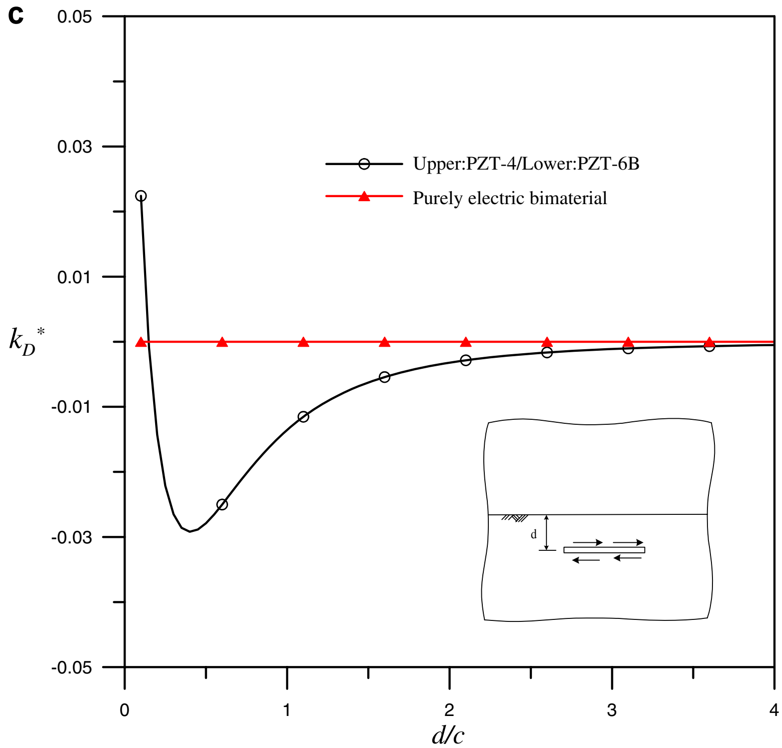

Fig. 3 (*continued*)

$$\boldsymbol{e}^{\mathrm{T}} = \begin{bmatrix} 0 & 0 & 0 & 0 & 0 & 13.4 \\ -6.98 & 13.8 & -6.98 & 0 & 0 & 0 \\ 0 & 0 & 0 & 13.4 & 0 & 0 \end{bmatrix} (\mathrm{Cm}^{-2}),$$

$$\boldsymbol{\alpha} = \begin{bmatrix} 60.0 & 0 & 0 \\ 0 & 54.7 & 0 \\ 0 & 0 & 60.0 \end{bmatrix} (10^{-10}\ \mathrm{CV}^{-1}\ \mathrm{m}^{-1}).$$

In our numerical investigations, the crack depth from the interface, i.e., d/c, is started from 0.1 and then increases with increment 0.05 until d/c is up to 4.0.

5.1. Half-plane with traction-free combined with various electric boundary conditions

Results for the half-plane with the mechanical traction-free condition combined with three different electric boundary conditions under uniform pressure, shear, and electric displacement loadings, respectively, are presented in Tables 1–3. Note that the case of the *electric-open* boundary condition has been studied by Yang et al. (2007).

(I) Under mechanical loadings: Let's consider the results listed in Tables 1 and 2 which are the cases under mechanical loadings. It can be observed that under mechanical loadings, the normalized mechanical stress intensity factors k_{I}^* and k_{II}^* for three different electric boundary conditions are very close to each other (see the data without parentheses). This implies that the effect of the type of the electric condition specified on the straight boundary is insignificant for the mechanical stress intensity factors when mechanical loadings are applied. Moreover, it is found that all the coupled mechanical–electric results are also very close to the results (data enclosed in parentheses) obtained using purely elastic analyses. Although present investigations are carried out only for the *horizontal* crack problem, a more general problem with cracks oriented *arbitrarily* studied by Yang (2008) does show that the observations made above are valid for problems with an arbitrary crack orientation. Note that the observations made above were also observed previously by Yang et al. (2007), but their results were only for the case of the electric-open problem with the crack's orientation embedded in the half-plane arbitrarily. In conclusion, present investigations show that the conclusions made by Yang et al. (2007) for the traction-free and electric-open case are still valid for other electric conditions specified on the boundary. Therefore we may strengthen their conclusion to state that the evaluations of the mechanical stress intensity factors under mechanical loadings for coupled mechanical and

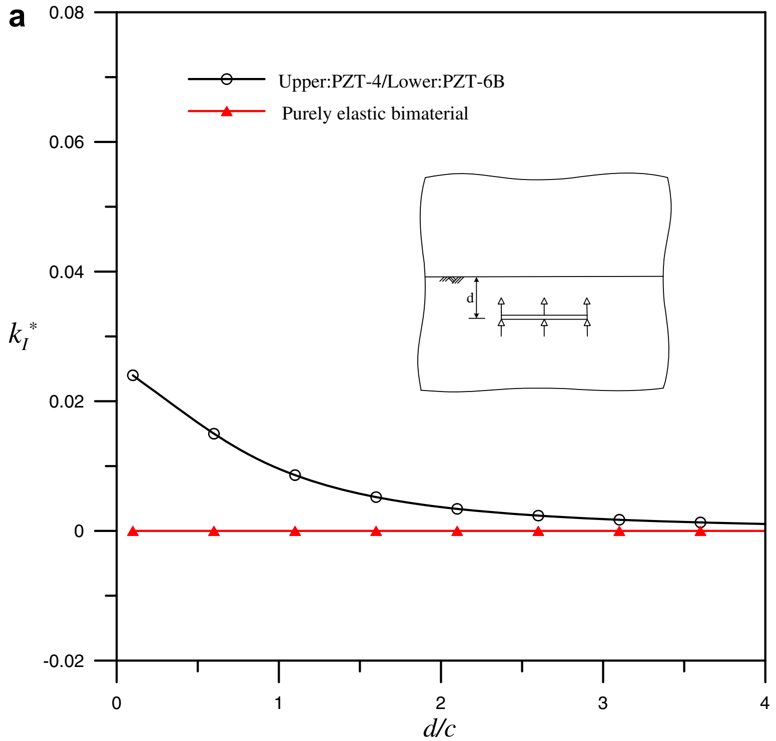

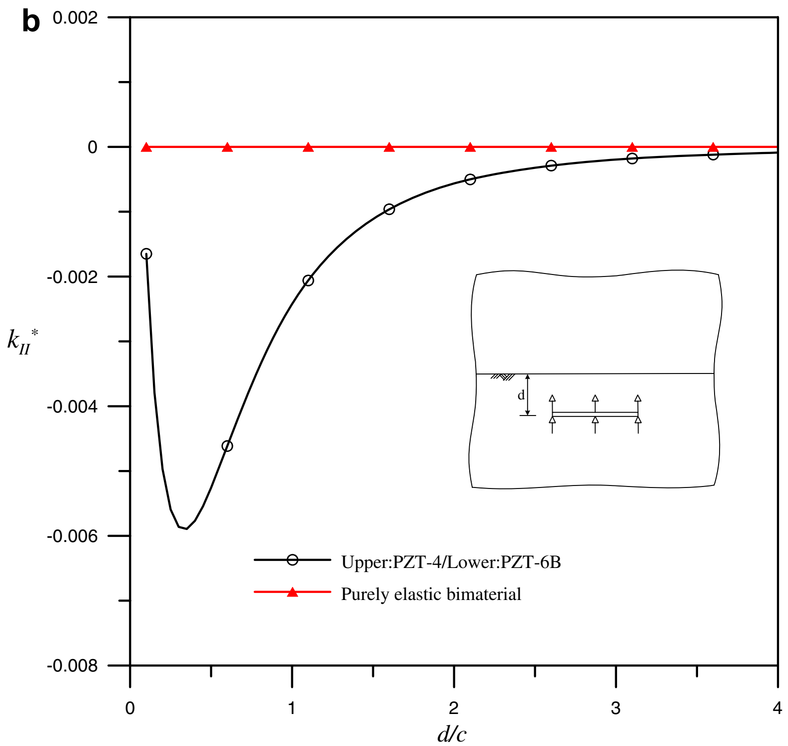

Fig. 4. Normalized generalized stress intensity factor (a) k_{I}^*, (b) k_{II}^* and (c) k_{D}^* for a piezoelectric bimaterial subjected to uniform electric displacement loading. The responses for the purely elastic bimaterial are also plotted.

electric problems may be evaluated directly by considering the corresponding decoupled (i.e., by letting $e_{kij} \equiv 0$) elastic problem irrespective of what electric boundary is applied on the boundary. In other words, for the half-plane

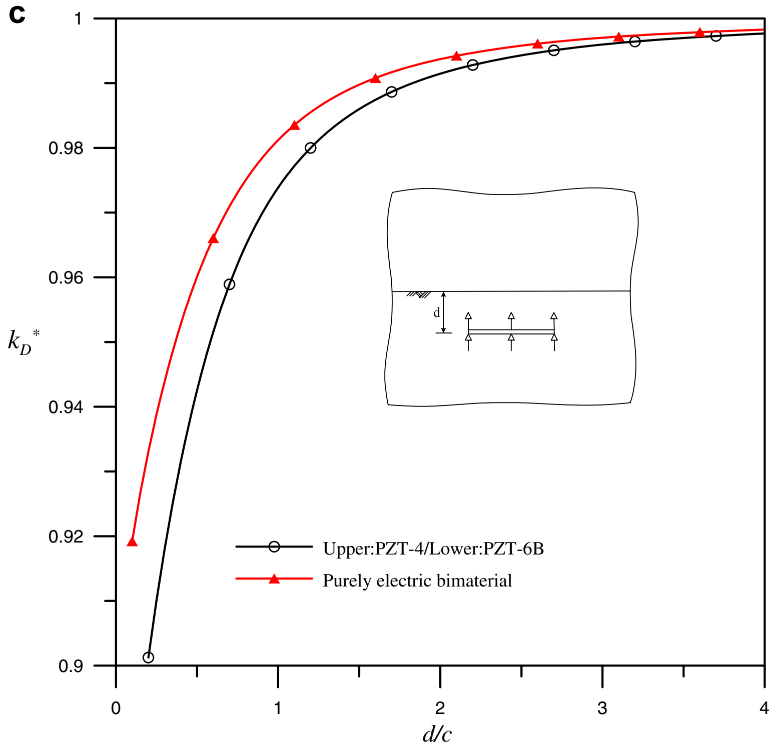

Fig. 4 (*continued*)

problem, the existence of the electric–mechanical coupling coefficients, i.e., e_{kij} and the electric boundary conditions both have little influence on the mechanical stress intensity factors under mechanical loadings. Now let's consider the direct piezoelectric effect, i.e, consider k_{D}^* induced by mechanical loadings. Contrary to the phenomenon just mentioned for mechanical stress intensity factors, the types of the electric conditions specified on the straight boundary, especially for the electric-closed case, do have some effect on the electric displacement intensity factor when mechanical loadings are applied, as can be observed in Tables 1 and 2.

(II) Under electric displacement loading: Table 3 shows the results when crack faces are subjected to electric displacement loading. Let's discuss the results for k_{D}^* first. It can be seen that for each electric boundary condition, the result obtained is close to the data enclosed in parentheses (obtained using purely electric analyses) if the same electric boundary condition is enforced. This implies that electric responses of piezoelectric materials induced by electric loading may be evaluated by considering the corresponding decoupled (i.e., by letting $e_{kij} \equiv 0$) electric problem with the same electric boundary applied on the boundary, a fact also observed by Yang et al. (2007) but only for the electric-open boundary condition. As to the normalized mechanical stress intensity factors k_{I}^* and k_{II}^* induced by electric displacement loading, i.e., considering the inverse piezoelectric effect, all small data for k_{I}^* and k_{II}^* shown in Table 3 show that the effect of electric displacement loading on mechanical stress intensity factors is insignificant, especially for the case of the electric-closed condition.

5.2. Half-plane with displacement-fixed combined with various electric boundary conditions

As discussed in the previous section, taking the elastic stiffness of the upper material to be a very large value allows the kernel functions for the problem of a half-plane with a mechanical displacement-fixed boundary to be obtained. Similar to the above discussions, three electric conditions may be enforced on the boundary. The results are shown in Tables 4–6.

(I) Under mechanical loadings: Tables 4 and 5 show the results for normalized mechanical stress intensity factors k_{I}^* and k_{II}^* induced by mechanical loadings for various electric boundary conditions. Comparing the results for the coupled condition with those for the decoupled case, almost the same conclusions made above for mechanical traction-free may be carried over to the mechanical displacement-fixed problem, i.e., the evaluations of the mechanical stress intensity factors under mechanical loadings for coupled mechanical and electric problems may be evaluated directly by considering the corresponding decoupled (i.e., by letting $e_{kij} \equiv 0$) elastic problem irrespective of what electric

boundary is applied on the boundary. However, the responses of k_{I}^* when d/c is small are slightly different under the electric-free condition and under applied shear loading. As to the k_{D}^* induced by mechanical loadings (i.e., direct piezoelectric effect) for displacement-fixed problems, it is found again that the type of electric conditions specified on the straight boundary do have some effect on the *electric displacement intensity factor*, as can be observed in Tables 4 and 5.

(II) Under electric displacement loading: Table 6 shows the results when crack faces are subjected to electric displacement loading. Let's again discuss the results for k_{D}^* first. It can also be seen that for each electric boundary condition, the result obtained is close to the data enclosed in parentheses (i.e., obtained using purely electric analyses) if the same electric boundary condition is enforced. Therefore, the conclusion for the traction-free problem made above for k_{D}^* induced by *electric loading* is still valid for the present case. As to the normalized *mechanical* stress intensity factors k_{I}^* and k_{II}^* induced by electric displacement loading, i.e, the inverse piezoelectric effect, all small data for k_{I}^* and k_{II}^* shown in Table 6 show again that the effect of electric displacement loading on *mechanical* stress intensity factors is insignificant, especially for the case of the electric-closed condition.

5.3. Piezoelectric bi-material problem

The validity of the decoupled purely elastic or purely electric analysis for piezoelectric half-plane problems with various electric conditions specified on the straight surface were addressed above. In this subsection, we consider a piezoelectric bimaterial composed of PZT-4 (arranged as the upper material or material 1) and PZT-6B (arranged as the lower material or material 2). As mentioned before, all the elastic and electric properties of the upper material affecting the behavior of the subinterface crack located in the lower material are in the matrix $\boldsymbol{F}$. To see whether or not the piezoelectric subinterface crack problem can be analyzed using the purely elastic bimaterial when mechanical stress intensity factors are concerned, or analyzed using the purely electric bimaterial when electric displacement intensity factor is concerned, the results of coupled and decoupled bimaterial problems are plotted in Fig. 2a–c, Fig. 3a–c, and Fig. 4a–c under uniform pressure, shear, and electric displacement loading, respectively. It can be observed that there is a discrepancy between the coupled and decoupled results for the normalized *mechanical* stress intensity factors k_{I}^* and k_{II}^* under *mechanical* loadings, as shown in Fig. 2(a and b) and Fig. 3(a and b). A discrepancy between the coupled and decoupled results for the normalized *electric displacement* intensity factor k_{D}^* under *electric displacement loading* is also found in Fig. 4c. Therefore, the analyses of the purely elastic bimaterial for the normalized *mechanical* stress intensity factors or the analysis of the purely electric bimaterial for the normalized *electric displacement* intensity factor is inadequate for piezoelectric bimaterial problems. The inadequateness can be seen with the error defined by

$$\text{Error} = \frac{\text{coupled result} - \text{decoupled result}}{\text{coupled result}} \times 100\%$$

where the percentage of error for the half-plane traction-free problem and for the piezoelectric bimaterial problem are shown in Tables 7–9 for $d/c = 0.4$. From these tables, we may conclude that for the effect of the bimaterial's constants on the subinterface crack, both elastic and electric properties should be taken into account for better accuracy of the generalized stress intensity factors. Note finally that this conclusion is also observed for many other piezoelectric bimaterials with different combinations, e.g., PZT-4/ PZT-5, PZT-4 /PZT-7, and PZT-4/BaTiO, although the results are not shown here (Yang, 2008).

6. Conclusions

The problem of a subinterface crack in an anisotropic piezoelectric bimaterial is formulated in terms of a system of singular integral equations for general anisotropic piezoelectric bimaterial. The kernel functions given in complex form for gen-

Table 7
Error of mechanical stress intensity factors computed using the coupled or decoupled (purely elastic) assumption for both half-plane and bimaterial problems with $d/c = 0.4$ (under uniform pressure loading)

SIF	Case	Half-plane with traction-free condition			Bimaterial
		$\boldsymbol{\alpha}^{(1)} = \boldsymbol{\alpha}_{Air}$ (electric-flux continuous)	$\boldsymbol{\alpha}^{(1)} \to \infty$ (electric closed)	$\boldsymbol{\alpha}^{(1)} = \boldsymbol{0}$ (electric-open)	PZT-4/PZT-6B
k_{I}^*	Coupled	2.8148	2.8320	2.8147	1.0101
	Decoupled	(2.8325)	(2.8325)	(2.8325)	(1.0840)
	Error (%)	−0.63	−0.02	−0.63	−7.32
k_{II}^*	Coupled	−0.8949	−0.8957	−0.8949	−0.0129
	Decoupled	(−0.8953)	(−0.8953)	(−0.8953)	(−0.0349)
	Error (%)	−0.04	0.04	−0.04	−170.54

Table 8
Error of mechanical stress intensity factors computed using the coupled or decoupled (purely elastic) assumption for both half-plane and bimaterial problems with $d/c = 0.4$ (under uniform shear loading)

SIF	Case	Half-plane with traction-free condition			Bimaterial
		$\boldsymbol{\alpha}^{(1)} = \boldsymbol{\alpha}_{Air}$ (electric-flux continuous)	$\boldsymbol{\alpha}^{(1)} \to \infty$ (electric closed)	$\boldsymbol{\alpha}^{(1)} = \boldsymbol{0}$ (electric-open)	PZT-4/PZT-6B
k_{I}^{*}	Coupled	0.3414	0.3411	0.3414	0.0171
	Decoupled	(0.3400)	(0.3400)	(0.3400)	0.0322
	Error (%)	0.41	0.32	0.41	−88.30
k_{II}^{*}	Coupled	1.0940	1.0954	1.0940	1.0073
	Decoupled	(1.0922)	(1.0922)	(1.0922)	(1.0152)
	Error (%)	0.16	0.29	0.16	−0.78

Table 9
Error of electric displacement intensity factor computed using the coupled or decoupled (purely electric) assumption for both half-plane and bimaterial problems with $d/c = 0.4$ (under uniform electric displacement loading)

SIF	Case	Half-plane with traction-free condition			Bimaterial
		$\boldsymbol{\alpha}^{(1)} = \boldsymbol{\alpha}_{Air}$ (electric-flux continuous)	$\boldsymbol{\alpha}^{(1)} \to \infty$ (electric closed)	$\boldsymbol{\alpha}^{(1)} = \boldsymbol{0}$ (electric-open)	PZT-4/PZT-6B
k_{D}^{*}	Coupled	1.2845	0.8407	1.2862	0.9315
	Decoupled	(1.2894)	(0.8370)	(1.2915)	(0.9528)
	Error (%)	−0.38	0.44	−0.41	−2.29

eral anisotropic piezoelectric bimaterial are developed in real forms for transversely isotropic piezoelectric bimaterial. The real kernel functions are decoupled into those for elastic bimaterial and electric bimaterial, respectively, when the piezoelectric-stress effects disappear. By considering certain special properties of one of the bimaterial, various real kernel functions are obtained for half-plane problems with various boundary conditions enforced for mechanical and electric fields. Investigations of a half-plane with various electric boundary conditions show that, particularly for mechanical traction-free half-plane problem, the evaluations of the mechanical stress intensity factors (electric displacement intensity factor) under mechanical loadings (electric displacement loading) for coupled mechanical and electric problems may be evaluated directly by considering the corresponding decoupled elastic (electric) problem irrespective of what electric boundary is applied on the boundary. However, for piezoelectric bimaterial, purely elastic bimaterial analysis or purely electric bimaterial analysis is inadequate for the determination of the generalized stress intensity factors. Instead, for better accuracy of the generalized stress intensity factors, both elastic and electric properties of the bimaterial's constants should be simultaneously taken into account.

Appendix A

The $\lambda_{\alpha}^{(j)} (\alpha = 1, 2, 3)$ in Eq. (4.6) are expressed as

$$\lambda_{\alpha}^{(j)} = -\frac{\beta_4 p_{\alpha}^{(j)^4} + \beta_2 p_{\alpha}^{(j)^2} + \beta_0}{\xi_4 p_{\alpha}^{(j)^4} + \xi_2 p_{\alpha}^{(j)^2} + \xi_0}, \quad (\alpha = 1, 2) \tag{A.1}$$

$$\lambda_{3}^{(j)} = \frac{\eta_3 p_{3}^{(j)^2} + \eta_1}{\zeta_5 p_{3}^{(j)^4} + \zeta_3 p_{3}^{(j)^2} + \zeta_1}, \tag{A.2}$$

where

$$\beta_4 = c_{22}^{(j)} e_{16}^{(j)} \alpha_{22}^{(j)} + e_{16}^{(j)} e_{22}^{(j)^2},$$
$$\beta_2 = c_{12}^{(j)} e_{22}^{(j)} \alpha_{11}^{(j)} + c_{44}^{(j)} e_{22}^{(j)} \alpha_{11}^{(j)} - c_{22}^{(j)} e_{21}^{(j)} \alpha_{11}^{(j)} - c_{12}^{(j)} e_{16}^{(j)} \alpha_{22}^{(j)} - e_{16}^{(j)} e_{22}^{(j)} e_{21}^{(j)} + e_{22}^{(j)} e_{16}^{(j)^2},$$
$$\beta_0 = -c_{44}^{(j)} e_{21}^{(j)} \alpha_{11}^{(j)} - e_{21}^{(j)} e_{16}^{(j)^2},$$
$$\xi_4 = c_{22}^{(j)} c_{44}^{(j)} \alpha_{22}^{(j)} + c_{44}^{(j)} e_{22}^{(j)^2},$$
$$\xi_2 = -c_{44}^{(j)} e_{22}^{(j)} e_{21}^{(j)} + c_{22}^{(j)} e_{21}^{(j)} e_{16}^{(j)} - c_{12}^{(j)} e_{22}^{(j)} e_{16}^{(j)} + c_{22}^{(j)} e_{16}^{(j)^2} + c_{22}^{(j)} c_{44}^{(j)} \alpha_{11}^{(j)} - c_{12}^{(j)} c_{44}^{(j)} \alpha_{22}^{(j)},$$
$$\xi_0 = -c_{44}^{(j)} c_{12}^{(j)} \alpha_{11}^{(j)} - c_{12}^{(j)} e_{16}^{(j)^2},$$
$$\eta_3 = c_{12}^{(j)} c_{44}^{(j)} e_{22}^{(j)} - c_{44}^{(j)} c_{22}^{(j)} e_{21}^{(j)},$$
$$\eta_1 = -c_{12}^{(j)^2} e_{16}^{(j)} + c_{11}^{(j)} c_{22}^{(j)} e_{16}^{(j)} + c_{12}^{(j)} c_{44}^{(j)} e_{21}^{(j)} - c_{11}^{(j)} c_{44}^{(j)} e_{22}^{(j)},$$

$$
\begin{aligned}
\zeta_5 &= c_{44}^{(j)} c_{22}^{(j)} \alpha_{22}^{(j)} + c_{44}^{(j)} e_{22}^{(j)^2}, \\
\zeta_3 &= c_{11}^{(j)} e_{22}^{(j)^2} + c_{22}^{(j)} e_{21}^{(j)^2} - c_{12}^{(j)^2} \alpha_{22}^{(j)} - c_{12}^{(j)} e_{22}^{(j)} e_{16}^{(j)} - 2c_{12}^{(j)} e_{21}^{(j)} e_{22}^{(j)} - 2c_{12}^{(j)} c_{44}^{(j)} \alpha_{22}^{(j)} + c_{11}^{(j)} c_{22}^{(j)} \alpha_{22}^{(j)} \\
&\quad + c_{22}^{(j)} e_{16}^{(j)} e_{21}^{(j)} - 2c_{44}^{(j)} e_{21}^{(j)} e_{22}^{(j)}, \\
\zeta_1 &= c_{44}^{(j)} e_{21}^{(j)^2} + c_{11}^{(j)} e_{22}^{(j)} e_{16}^{(j)} + c_{11}^{(j)} c_{44}^{(j)} \alpha_{22}^{(j)} - c_{12}^{(j)} e_{21}^{(j)} e_{16}^{(j)}.
\end{aligned}
\tag{A.3}
$$

Appendix B

$Y_{\alpha\beta}^{(j)}$ and $\widehat{Y}_{\alpha\beta}^{(j)}$ (α, β = 1, 2, 3) in Eq. (4.7) are expressed as

$$
\begin{aligned}
Y_{11}^{(j)} &= i[(1+\lambda_2^{(j)}\lambda_3^{(j)})a_{11} - (1+\lambda_1^{(j)}\lambda_3^{(j)})a_{12} + (\lambda_1^{(j)} - \lambda_2^{(j)})a_{13}]/|\boldsymbol{B}^{(j)}|, \\
Y_{22}^{(j)} &= i[(p_2^{(j)} + \lambda_2^{(j)}\lambda_3^{(j)}p_3^{(j)})a_{21} - (p_1^{(j)} + \lambda_1^{(j)}\lambda_3^{(j)}p_3^{(j)})a_{22} + (\lambda_1^{(j)}p_2^{(j)} - \lambda_2^{(j)}p_1^{(j)})a_{23}]/|\boldsymbol{B}^{(j)}|, \\
Y_{33}^{(j)} &= i[p_1^{(j)}(\lambda_3^{(j)}a_{32} - a_{33}) + p_2^{(j)}(a_{33} - \lambda_3^{(j)}a_{31}) + p_3^{(j)}\lambda_3^{(j)}(a_{31} - a_{32})]/|\boldsymbol{B}^{(j)}|, \\
Y_{23}^{(j)} &= i[p_1^{(j)}(\lambda_3^{(j)}a_{22} - a_{23}) + p_2^{(j)}(a_{23} - \lambda_3^{(j)}a_{21}) + p_3^{(j)}\lambda_3^{(j)}(a_{21} - a_{22})]/|\boldsymbol{B}^{(j)}|, \\
\widehat{Y}_{12}^{(j)} &= i[-\mathrm{Im}\{p_1^{(j)}\}(a_{12} + \lambda_2^{(j)}a_{13}) + \mathrm{Im}\{p_2^{(j)}\}(a_{11} + \lambda_1^{(j)}a_{13}) + \mathrm{Im}\{p_3^{(j)}\}\lambda_3^{(j)}(\lambda_2^{(j)}a_{11} - \lambda_1^{(j)}a_{12})]/|\boldsymbol{B}^{(j)}|, \\
\widehat{Y}_{13}^{(j)} &= i[-\mathrm{Im}\{p_1^{(j)}\}(a_{13} - \lambda_3^{(j)}a_{12}) + \mathrm{Im}\{p_2^{(j)}\}(a_{13} - \lambda_3^{(j)}a_{11}) + \mathrm{Im}\{p_3^{(j)}\}\lambda_3^{(j)}(a_{11} - a_{12})]/|\boldsymbol{B}^{(j)}|,
\end{aligned}
\tag{B.1}
$$

where

$$|\boldsymbol{B}^{(j)}| = i[\lambda_1^{(j)}\lambda_3^{(j)}\mathrm{Im}\{p_2^{(j)} - p_3^{(j)}\} + \lambda_2^{(j)}\lambda_3^{(j)}\mathrm{Im}\{p_3^{(j)} - p_1^{(j)}\} + \mathrm{Im}\{p_2^{(j)} - p_1^{(j)}\}],$$

for type I roots and

$$
\begin{aligned}
Y_{11}^{(j)} &= -2[\mathrm{Im}\{a_{11}\} + \lambda_3^{(j)}\mathrm{Im}\{a_{11}\bar{\lambda}_1^{(j)}\} + a_{13}\mathrm{Im}\{\lambda_1^{(j)}\}]/|\boldsymbol{B}^{(j)}|, \\
Y_{22}^{(j)} &= -2[\lambda_3^{(j)}\mathrm{Im}\{p_3^{(j)}\}\mathrm{Re}\{\bar{\lambda}_1^{(j)}a_{21}\} - \mathrm{Im}\{\bar{p}_1^{(j)}a_{21}\} - \mathrm{Im}\{a_{23}\}\mathrm{Re}\{p_1^{(j)}\bar{\lambda}_1^{(j)}\}]/|\boldsymbol{B}^{(j)}|, \\
Y_{33}^{(j)} &= -2[\lambda_3^{(j)}\mathrm{Im}\{a_{31}\bar{p}_1^{(j)}\} + \lambda_3^{(j)}\mathrm{Im}\{p_3^{(j)}\}\mathrm{Re}\{a_{31}\} - \mathrm{Im}\{a_{33}\}\mathrm{Re}\{p_1^{(j)}\}]/|\boldsymbol{B}^{(j)}|, \\
Y_{23}^{(j)} &= -2[\lambda_3^{(j)}\mathrm{Im}\{a_{21}\bar{p}_1^{(j)}\} + \lambda_3^{(j)}\mathrm{Im}\{p_3^{(j)}\}\mathrm{Re}\{a_{21}\} - \mathrm{Im}\{a_{23}\}\mathrm{Re}\{p_1^{(j)}\}]/|\boldsymbol{B}^{(j)}|, \\
\widehat{Y}_{12}^{(j)} &= -2[\mathrm{Re}\{a_{11}\bar{p}_1^{(j)}\} + \lambda_3\mathrm{Im}\{p_3^{(j)}\}\mathrm{Im}\{a_{11}\bar{\lambda}_1^{(j)}\} + a_{13}\mathrm{Re}\{\bar{p}_1^{(j)}\lambda_1^{(j)}\}]/|\boldsymbol{B}^{(j)}|, \\
\widehat{Y}_{13}^{(j)} &= 2[\lambda_3^{(j)}\mathrm{Re}\{a_{11}\bar{p}_1^{(j)}\} - \lambda_3^{(j)}\mathrm{Im}\{p_3^{(j)}\}\mathrm{Im}\{a_{11}\} - a_{13}\mathrm{Re}\{p_1^{(j)}\}]/|\boldsymbol{B}^{(j)}|,
\end{aligned}
\tag{B.2}
$$

where

$$|\boldsymbol{B}^{(j)}| = -2[\lambda_3^{(j)}(\mathrm{Re}\{\lambda_1^{(j)}\bar{p}_1^{(j)}\} - \mathrm{Im}\{p_3^{(j)}\}\mathrm{Im}\{\lambda_1^{(j)}\}) + \mathrm{Re}\{p_1^{(j)}\}]$$

for type II roots. The a_{jk}, (j, k = 1, 2, 3) appearing in Eqs. (B.1) and (B.2) are defined as

$$
\begin{aligned}
a_{1k} &= [\kappa_{11}(p_k^{(j)})\lambda_k^{(j)} + \kappa_{10}(p_k^{(j)})]/\Delta(p_k^{(j)}), \\
a_{2k} &= [\kappa_{21}(p_k^{(j)})\lambda_k^{(j)} + \kappa_{20}(p_k^{(j)})]/\Delta(p_k^{(j)}), \quad (k = 1, 2), \\
a_{3k} &= [\kappa_{31}(p_k^{(j)})\lambda_k^{(j)} + \kappa_{30}(p_k^{(j)})]/\Delta(p_k^{(j)}), \\
a_{13} &= [-\kappa_{11}(p_3^{(j)}) + \lambda_3^{(j)}\kappa_{10}(p_3^{(j)})]/\Delta(p_3^{(j)}), \\
a_{23} &= [-\kappa_{21}(p_3^{(j)}) + \lambda_3^{(j)}\kappa_{20}(p_3^{(j)})]/\Delta(p_3^{(j)}), \\
a_{33} &= [-\kappa_{31}(p_3^{(j)}) + \lambda_3^{(j)}\kappa_{30}(p_3^{(j)})]/\Delta(p_3^{(j)}),
\end{aligned}
\tag{B.3}
$$

where

$$
\begin{aligned}
\kappa_{11}(p_k^{(j)}) &= (c_{22}^{(j)}e_{16}^{(j)} - c_{44}^{(j)}e_{22}^{(j)})p_k^{(j)}, \\
\kappa_{10}(p_k^{(j)}) &= (c_{22}^{(j)}\alpha_{22}^{(j)} + e_{22}^{(j)^2})p_k^{(j)^3} + (c_{44}^{(j)}\alpha_{22}^{(j)} + e_{22}^{(j)}e_{16}^{(j)})p_k^{(j)}, \\
\kappa_{21}(p_k^{(j)}) &= c_{44}^{(j)}e_{22}^{(j)}p_k^{(j)^2} - c_{12}^{(j)}e_{16}^{(j)}, \\
\kappa_{20}(p_k^{(j)}) &= -(c_{12}^{(j)}\alpha_{22}^{(j)} + e_{22}^{(j)}e_{21}^{(j)} + c_{44}^{(j)}\alpha_{22}^{(j)})p_k^{(j)^2} - e_{21}^{(j)}e_{16}^{(j)}, \\
\kappa_{31}(p_k^{(j)}) &= -c_{22}^{(j)}c_{44}^{(j)}p_k^{(j)^2} + c_{44}^{(j)}c_{12}^{(j)}, \\
\kappa_{30}(p_k^{(j)}) &= (c_{22}^{(j)}e_{21}^{(j)} - c_{12}^{(j)}e_{22}^{(j)} - c_{44}^{(j)}e_{22}^{(j)})p_k^{(j)^2} + c_{44}^{(j)}e_{21}^{(j)}, \\
\Delta(p_k^{(j)}) &= -p_k^{(j)}[(c_{22}^{(j)}c_{44}^{(j)}\alpha_{22}^{(j)} + c_{44}^{(j)}e_{22}^{(j)^2})p_k^{(j)^2} + (c_{22}^{(j)}e_{21}^{(j)}e_{16}^{(j)} - c_{44}^{(j)}e_{21}^{(j)}e_{22}^{(j)} - c_{12}^{(j)}e_{22}^{(j)}e_{16}^{(j)} - c_{44}^{(j)}c_{12}^{(j)}\alpha_{22}^{(j)})],
\end{aligned}
\tag{B.4}
$$

Appendix C

The kernel functions for which lower material belongs to type I roots are:

$$
\begin{aligned}
K_j^{11} &= V_{j1}[(V_{11}n_1^{(2)}r_{1j} + V_{21}n_2^{(2)}r_{2j} + V_{31}n_3^{(2)}r_{3j}\lambda_3^{(2)})(F_{12} + F_{11}n_j^{(2)} - F_{13}\lambda_j^{(2)}) \\
&\quad + (V_{12}n_1^{(2)}r_{1j} + V_{22}n_2^{(2)}r_{2j} + V_{32}n_3^{(2)}r_{3j}\lambda_3^{(2)})(F_{22} - F_{21}n_j^{(2)} - F_{23}\lambda_j^{(2)}) \\
&\quad + (V_{13}n_1^{(2)}r_{1j} + V_{23}n_2^{(2)}r_{2j} + V_{33}n_3^{(2)}r_{3j}\lambda_3^{(2)})(F_{32} - F_{31}n_j^{(2)} - F_{33}\lambda_j^{(2)})], \\
K_j^{12} &= V_{j2}[(V_{11}n_1^{(2)}q_{1j} + V_{21}n_2^{(2)}q_{2j} + V_{31}n_3^{(2)}q_{3j}\lambda_3^{(2)})(F_{12} + F_{11}n_j^{(2)} - F_{13}\lambda_j^{(2)}) \\
&\quad + (V_{12}n_1^{(2)}q_{1j} + V_{22}n_2^{(2)}q_{2j} + V_{32}n_3^{(2)}q_{3j}\lambda_3^{(2)})(F_{22} - F_{21}n_j^{(2)} - F_{23}\lambda_j^{(2)}) \\
&\quad + (V_{13}n_1^{(2)}q_{1j} + V_{23}n_2^{(2)}q_{2j} + V_{33}n_3^{(2)}q_{3j}\lambda_3^{(2)})(F_{32} - F_{31}n_j^{(2)} - F_{33}\lambda_j^{(2)})], \\
K_j^{21} &= -V_{j1}[(V_{11}q_{1j} + V_{21}q_{2j} + V_{31}q_{3j}\lambda_3^{(2)})(F_{12} + F_{11}n_j^{(2)} - F_{13}\lambda_j^{(2)}) \\
&\quad + (V_{12}q_{1j} + V_{22}q_{2j} + V_{32}q_{3j}\lambda_3^{(2)})(F_{22} - F_{21}n_j^{(2)} - F_{23}\lambda_j^{(2)}) \\
&\quad + (V_{13}q_{1j} + V_{23}q_{2j} + V_{33}q_{3j}\lambda_3^{(2)})(F_{32} - F_{31}n_j^{(2)} - F_{33}\lambda_j^{(2)})], \\
K_j^{22} &= V_{j2}[(V_{11}r_{1j} + V_{21}r_{2j} + V_{31}r_{3j}\lambda_3^{(2)})(F_{12} + F_{11}n_j^{(2)} - F_{13}\lambda_j^{(2)}) \\
&\quad + (V_{12}r_{1j} + V_{22}r_{2j} + V_{32}r_{3j}\lambda_3^{(2)})(F_{22} - F_{21}n_j^{(2)} - F_{23}\lambda_j^{(2)}) \\
&\quad + (V_{13}r_{1j} + V_{23}r_{2j} + V_{33}r_{3j}\lambda_3^{(2)})(F_{32} - F_{31}n_j^{(2)} - F_{33}\lambda_j^{(2)})], \\
K_j^{31} &= V_{j1}[(V_{11}q_{1j}\lambda_1^{(2)} + V_{21}q_{2j}\lambda_2^{(2)} - V_{31}q_{3j})(F_{12} + F_{11}n_j^{(2)} - F_{13}\lambda_j^{(2)}) \\
&\quad + (V_{12}q_{1j}\lambda_1^{(2)} + V_{22}q_{2j}\lambda_2^{(2)} - V_{32}q_{3j})(F_{22} - F_{21}n_j^{(2)} - F_{23}\lambda_j^{(2)}) \\
&\quad + (V_{13}q_{1j}\lambda_1^{(2)} + V_{23}q_{2j}\lambda_2^{(2)} - V_{33}q_{3j})(F_{32} - F_{31}n_j^{(2)} - F_{33}\lambda_j^{(2)})], \\
K_j^{32} &= -V_{j2}[(V_{11}r_{1j}\lambda_1^{(2)} + V_{21}r_{2j}\lambda_2^{(2)} - V_{31}r_{3j})(F_{12} + F_{11}n_j^{(2)} - F_{13}\lambda_j^{(2)}) \\
&\quad + (V_{12}r_{1j}\lambda_1^{(2)} + V_{22}r_{2j}\lambda_2^{(2)} - V_{32}r_{3j})(F_{22} - F_{21}n_j^{(2)} - F_{23}\lambda_j^{(2)}) \\
&\quad + (V_{13}r_{1j}\lambda_1^{(2)} + V_{23}r_{2j}\lambda_2^{(2)} - V_{33}r_{3j})(F_{32} - F_{31}n_j^{(2)} - F_{33}\lambda_j^{(2)})], \\
K_3^{11} &= V_{31}\{(V_{11}n_1^{(2)}r_{31} + V_{21}n_2^{(2)}r_{23} + V_{31}n_3^{(2)}r_{33}\lambda_3^{(2)})[F_{13} + (F_{12} + F_{11}n_3^{(2)})\lambda_3^{(2)}] \\
&\quad + (V_{12}n_1^{(2)}r_{13} + V_{22}n_2^{(2)}r_{23} + V_{32}n_3^{(2)}r_{33}\lambda_3^{(2)})[F_{23} + (F_{22} - F_{21}n_3^{(2)})\lambda_3^{(2)}] \\
&\quad + (V_{13}n_1^{(2)}r_{13} + V_{23}n_2^{(2)}r_{23} + V_{33}n_3^{(2)}r_{33}\lambda_3^{(2)})[F_{33} + (F_{32} - F_{31}n_3^{(2)})\lambda_3^{(2)}]\}, \\
K_3^{12} &= V_{32}\{(V_{11}n_1^{(2)}q_{13} + V_{21}n_2^{(2)}q_{23} + V_{31}n_3^{(2)}q_{33}\lambda_3^{(2)})[F_{13} + (F_{12} + F_{11}n_3^{(2)})\lambda_3^{(2)}] \\
&\quad + (V_{12}n_1^{(2)}q_{13} + V_{22}n_2^{(2)}q_{23} + V_{32}n_3^{(2)}q_{33}\lambda_3^{(2)})[F_{23} + (F_{22} - F_{21}n_3^{(2)})\lambda_3^{(2)}] \\
&\quad + (V_{13}n_1^{(2)}q_{13} + V_{23}n_2^{(2)}q_{23} + V_{33}n_3^{(2)}q_{33}\lambda_3^{(2)})[F_{33} + (F_{32} - F_{31}n_3^{(2)})\lambda_3^{(2)}]\}, \\
K_3^{21} &= -V_{31}\{(V_{11}q_{13} + V_{21}q_{23} + V_{31}q_{33}\lambda_3^{(2)})[F_{13} + (F_{12} + F_{11}n_3^{(2)})\lambda_3^{(2)}] \\
&\quad + (V_{12}q_{13} + V_{22}q_{23} + V_{32}q_{33}\lambda_3^{(2)})[F_{23} + (F_{22} - F_{21}n_3^{(2)})\lambda_3^{(2)}] \\
&\quad + (V_{13}q_{13} + V_{23}q_{23} + V_{33}q_{33}\lambda_3^{(2)})[F_{33} + (F_{32} - F_{31}n_3^{(2)})\lambda_3^{(2)}]\}, \\
K_3^{22} &= V_{32}\{(V_{11}r_{13} + V_{21}r_{23} + V_{31}r_{33}\lambda_3^{(2)})[F_{13} + (F_{12} + F_{11}n_3^{(2)})\lambda_3^{(2)}] \\
&\quad + (V_{12}r_{13} + V_{22}r_{23} + V_{32}r_{33}\lambda_3^{(2)})[F_{23} + (F_{22} - F_{21}n_3^{(2)})\lambda_3^{(2)}] \\
&\quad + (V_{13}r_{13} + V_{23}r_{23} + V_{33}r_{33}\lambda_3^{(2)})[F_{33} + (F_{32} - F_{31}n_3^{(2)})\lambda_3^{(2)}]\}, \\
K_3^{31} &= V_{31}\{(V_{11}q_{13}\lambda_1^{(2)} + V_{21}q_{23}\lambda_2^{(2)} - V_{31}q_{33})[F_{13} + (F_{12} + F_{11}n_3^{(2)})\lambda_3^{(2)}] \\
&\quad + (V_{12}q_{13}\lambda_1^{(2)} + V_{22}q_{23}\lambda_2^{(2)} - V_{32}q_{33})[F_{23} + (F_{22} - F_{21}n_3^{(2)})\lambda_3^{(2)}] \\
&\quad + (V_{13}q_{13}\lambda_1^{(2)} + V_{23}q_{23}\lambda_2^{(2)} - V_{33}q_{33})[F_{33} + (F_{32} - F_{31}n_3^{(2)})\lambda_3^{(2)}]\}, \\
K_3^{32} &= -V_{32}\{(V_{11}r_{13}\lambda_1^{(2)} + V_{21}r_{23}\lambda_2^{(2)} - V_{31}r_{33})[F_{13} + (F_{12} + F_{11}n_3^{(2)})\lambda_3^{(2)}] \\
&\quad + (V_{12}r_{13}\lambda_1^{(2)} + V_{22}r_{23}\lambda_2^{(2)} - V_{23}r_{33})[F_{23} + (F_{22} - F_{21}n_3^{(2)})\lambda_3^{(2)}] \\
&\quad + (V_{13}r_{13}\lambda_1^{(2)} + V_{32}r_{23}\lambda_2^{(2)} - V_{33}r_{33})[F_{33} + (F_{32} - F_{31}n_3^{(2)})\lambda_3^{(2)}]\}, \\
K_j^{13} &= \frac{V_{j3}}{V_{j2}}K_j^{12}, \quad K_j^{23} = \frac{V_{j3}}{V_{j2}}K_j^{22}, \quad K_j^{33} = \frac{V_{j3}}{V_{j2}}K_j^{32}, \quad (j = 1, 2, 3),
\end{aligned}
\tag{C.1}
$$

where $V_{ij}(i, j = 1, 2, 3)$ are the elements of matrix $\boldsymbol{V}$ with the explicit expressions shown below

$$
\boldsymbol{V} = \begin{bmatrix} 1 + \lambda_2^{(2)}\lambda_3^{(2)} & n_2^{(2)} + n_3^{(2)}\lambda_2^{(2)}\lambda_3^{(2)} & \lambda_3^{(2)}(n_3^{(2)} - n_2^{(2)}) \\ -(1 + \lambda_1^{(2)}\lambda_3^{(2)}) & -(n_1^{(2)} + n_3^{(2)}\lambda_1^{(2)}\lambda_3^{(2)}) & \lambda_3^{(2)}(n_1^{(2)} - n_3^{(2)}) \\ \lambda_1^{(2)} - \lambda_2^{(2)} & n_2^{(2)}\lambda_1^{(2)} - n_1^{(2)}\lambda_2^{(2)} & n_2^{(2)} - n_1^{(2)} \end{bmatrix},
$$

Appendix D

The kernel functions for which lower material belongs to type II roots are

$$
\begin{aligned}
K_1^{\alpha\beta} &= F_{23}U_{3\beta}X_1^{\alpha2} + F_{33}U_{3\beta}X_1^{\alpha3} - F_{21}X_1^{\alpha2}\widehat{U}_{1\beta} - F_{31}X_1^{\alpha3}\widehat{U}_{1\beta} - X_1^{\alpha1}(F_{12}\widehat{U}_{2\beta} + F_{13}\widehat{U}_{3\beta}) \\
&\quad - F_{13}U_{3\beta}\widehat{X}_1^{\alpha1} + U_{2\beta}(F_{32}X_1^{\alpha3} - F_{12}\widehat{X}_1^{\alpha1}) + F_{11}(U_{1\beta}X_1^{\alpha1} - \widehat{U}_{1\beta}\widehat{X}_1^{\alpha1}) - F_{21}U_{1\beta}\widehat{X}_1^{\alpha2} \\
&\quad - F_{23}\widehat{U}_{3\beta}\widehat{X}_1^{\alpha2} + F_{22}(U_{2\beta}X_1^{\alpha2} - \widehat{U}_{2\beta}\widehat{X}_1^{\alpha2}) - \widehat{X}_1^{\alpha3}(F_{31}U_{1\beta} + F_{32}\widehat{U}_{2\beta} + F_{33}\widehat{U}_{3\beta}), \\
K_2^{\alpha\beta} &= J_{\alpha\beta}\{-F_{23}U_{3\beta}X_2^{\alpha2} - F_{33}U_{3\beta}X_2^{\alpha3} + F_{21}X_2^{\alpha2}\widehat{U}_{1\beta} + F_{31}X_2^{\alpha3}\widehat{U}_{1\beta} - X_2^{\alpha1}(F_{12}\widehat{U}_{2\beta} + F_{13}\widehat{U}_{3\beta}) \\
&\quad + F_{13}U_{3\beta}\widehat{X}_2^{\alpha1} + U_{2\beta}(-F_{32}X_2^{\alpha3} + F_{12}\widehat{X}_2^{\alpha1}) + F_{11}(U_{1\beta}X_2^{\alpha1} + \widehat{U}_{1\beta}\widehat{X}_2^{\alpha1}) - F_{21}U_{1\beta}\widehat{X}_2^{\alpha2} \\
&\quad - F_{23}\widehat{U}_{3\beta}\widehat{X}_2^{\alpha2} - F_{22}(U_{2\beta}X_2^{\alpha2} + \widehat{U}_{2\beta}\widehat{X}_2^{\alpha2}) - \widehat{X}_2^{\alpha3}(F_{31}U_{1\beta} + F_{32}\widehat{U}_{2\beta} + F_{33}\widehat{U}_{3\beta})\}, \\
K_3^{\alpha1} &= 2\hat{q}\{\lambda_3^{(2)}[\widehat{X}_3^{\alpha2}(F_{22} - F_{21}n_3^{(2)}) + \widehat{X}_3^{\alpha3}(F_{32} - F_{31}n_3^{(2)})] + F_{23}\widehat{X}_3^{\alpha2} + F_{33}\widehat{X}_3^{\alpha3} \\
&\quad + X_3^{\alpha1}[F_{13} + \lambda_3^{(2)}(F_{12} + F_{11}n_3^{(2)})]\}, \\
K_3^{\alpha2} &= -2(\hat{q}n_1^{(2)} + m_1^{(2)}\hat{r})\{\lambda_3[X_3^{\alpha2}(F_{22} - F_{21}n_3^{(2)}) + X_3^{\alpha3}(F_{32} - F_{31}n_3^{(2)})] + F_{23}X_3^{\alpha2} + F_{33}X^{\alpha3} \\
&\quad - \widehat{X}_3^{\alpha1}[F_{13} + \lambda_3^{(2)}(F_{12} + F_{11}n_3^{(2)})]\}, \\
K_3^{\alpha3} &= \frac{m_1^{(2)}}{(n_1^{(2)}\hat{q} + m_1^{(2)}\hat{r})}K_3^{\alpha2},
\end{aligned}
\tag{D.1}
$$

where

$$
\begin{aligned}
X_j^{11} &= -\lambda_3^{(2)}\{\hat{q}[n_1^{(2)}(r_{1j} + r_{2j}) - 2n_3^{(2)}r_{3j}] - n_1^{(2)}\hat{r}(q_{1j} - q_{2j}) + m_1^{(2)}[\hat{q}(q_{1j} - q_{2j}) + \hat{r}(r_{1j} + r_{2j})]\} \\
&\quad + n_1^{(2)}(q_{1j} - q_{2j}) - m_1^{(2)}(r_{1j} + r_{2j}), \\
X_j^{12} &= n_3^{(2)}\lambda_3^{(2)}\{\hat{q}[n_1^{(2)}(q_{1j} + q_{2j} - 2q_{3j}) - m_1^{(2)}(r_{1j} - r_{2j})] + [m_1^{(2)}(q_{1j} + q_{2j} - 2q_{3j}) + n_1^{(2)}\hat{r}(r_{1j} - r_{2j})]\} \\
&\quad + (m_1^{(2)^2} + n_1^{(2)^2})(r_{1j} - r_{2j}), \\
X_j^{13} &= \lambda_3^{(2)}\{m_1^{(2)}n_3^{(2)}(q_{1j} + q_{2j} - 2q_{3j}) - m_1^{(2)^2}(r_{1j} - r_{2j}) - n_1^{(2)}(n_1^{(2)} - n_3^{(2)})(r_{1j} - r_{2j})\}, \\
X_j^{21} &= r_{1j} - r_{2j} + \lambda_3^{(2)}[\hat{q}(q_{1j} + q_{2j} - 2q_{3j}) + \hat{r}(r_{1j} - r_{2j})], \\
X_j^{22} &= \hat{r}\lambda_3^{(2)}[-n_3^{(2)}(q_{1j} - q_{2j}) - 2m_1^{(2)}r_{3j}] - (r_{1j} + r_{2j})(m_1^{(2)} - \hat{q}n_3^{(2)}\lambda_3^{(2)}) + n_1^{(2)}(-q_{1j} + q_{2j} - 2\hat{q}r_{3j}\lambda_3^{(2)}), \\
X_j^{23} &= \lambda_3^{(2)}[(n_1^{(2)} - n_3^{(2)})(q_{1j} - q_{2j}) + m_1^{(2)}(r_{1j} + r_{2j} - 2r_{3j})], \\
X_j^{31} &= \hat{q}(q_{1j} + q_{2j} - 2q_{3j}) - \hat{r}(r_{1j} - r_{2j}) - \lambda_3^{(2)}(r_{1j} - r_{2j})(\hat{q}^2 + \hat{r}^2), \\
X_j^{32} &= n_1^{(2)}[\hat{q}(r_{1j} + r_{2j} - 2r_{3j}) + \hat{r}(q_{1j} - q_{2j})] + m_1^{(2)}[-\hat{q}(q_{1j} - q_{2j}) + \hat{r}(r_{1j} + r_{2j} - 2r_{3j})] \\
&\quad + n_3^{(2)}\lambda_3^{(2)}(q_{1j} - q_{2j})(\hat{q}^2 + \hat{r}^2), \\
X_j^{33} &= -(n_1^{(2)} - n_3^{(2)})\lambda_3^{(2)}[\hat{q}(r_{1j} + r_{2j}) + \hat{r}(q_{1j} - q_{2j})] - m_1^{(2)}\{2r_{3j} - \lambda_3^{(2)}[\hat{q}(q_{1j} - q_{2j}) - \hat{r}(r_{1j} + r_{2j})]\}, \\
\widehat{X}_j^{11} &= -\lambda_3^{(2)}\{\hat{q}[n_1^{(2)}(q_{1j} + q_{2j}) - 2n_3^{(2)}q_{3j}m_1(r_{1j} - r_{2j})] + \hat{r}[m_1^{(2)}(q_{1j} + q_{2j}) + n_1^{(2)}(r_{1j} - r_{2j})]\} \\
&\quad - m_1^{(2)}(q_{1j} + q_{2j}) - n_1^{(2)}(r_{1j} - r_{2j}), \\
\widehat{X}_j^{12} &= -n_3^{(2)}\lambda_3^{(2)}\{n_1^{(2)}[\hat{q}(r_{1j} + r_{2j} - 2r_{3j}) - \hat{r}(q_{1j} - q_{2j})] + m_1^{(2)}[\hat{q}(q_{1j} - q_{2j}) + \hat{r}(r_{1j} + r_{2j} - 2r_{3j})]\} \\
&\quad + (m_1^{(2)^2} + n_1^{(2)^2})(q_{1j} - q_{2j}), \\
\widehat{X}_j^{13} &= -\lambda_3^{(2)}[m_1^{(2)^2}(q_{1j} - q_{2j}) + n_1^{(2)}(n_1^{(2)} - n_3^{(2)})(q_{1j} - q_{2j}) + m_1^{(2)}n_3^{(2)}(r_{1j} + r_{2j} - 2r_{3j})], \\
\widehat{X}_j^{21} &= q_{1j} - q_{2j} - \lambda_3^{(2)}[\hat{q}(r_{1j} + r_{2j} - 2r_{3j}) + \hat{r}(-q_{1j} + q_{2j})], \\
\widehat{X}_j^{22} &= n_3^{(2)}\lambda_3^{(2)}[\hat{q}(q_{1j} + q_{2j}) + \hat{r}(r_{1j} - r_{2j})] + n_1^{(2)}(r_{1j} - r_{2j} - 2\hat{q}q_{3j}\lambda_3) - m_1^{(2)}(q_{1j} + q_{2j} + 2q_{3j}\hat{r}\lambda_3^{(2)}), \\
\widehat{X}_j^{23} &= \lambda_3^{(2)}[m_1^{(2)}(q_{1j} + q_{2j} - 2q_{3j}) - (n_1^{(2)} - n_3^{(2)})(r_{1j} - r_{2j})], \\
\widehat{X}_j^{31} &= -\hat{q}(r_{1j} + r_{2j} - 2r_{3j}) - \hat{r}(q_{1j} - q_{2j}) - \lambda_3^{(2)}(q_{1j} - q_{2j})(\hat{q}^2 + \hat{r}^2), \\
\widehat{X}_j^{32} &= \hat{q}[n_1^{(2)}(q_{1j} + q_{2j} - 2q_{3j}) + m_1^{(2)}(r_{1j} - r_{2j})] - \hat{q}n_3^{(2)}\lambda_3^{(2)}(r_{1j} - r_{2j}) \\
&\quad + \hat{r}[m_1^{(2)}(q_{1j} + q_{2j} - 2q_{3j}) - (r_{1j} - r_{2j})(n_1^{(2)} + n_3^{(2)}\hat{r}\lambda_3^{(2)})], \\
\widehat{X}_j^{33} &= -\lambda_3^{(2)}(n_1^{(2)} - n_3^{(2)})[\hat{q}(q_{1j} + q_{2j}) - \hat{r}(r_{1j} - r_{2j})] - m_1^{(2)}\{2q_{3j} + \lambda_3^{(2)}[\hat{q}(r_{1j} - r_{2j}) + \hat{r}(q_{1j} + q_{2j})]\},
\end{aligned}
\tag{D.2}
$$

and $J_{\alpha\beta}$, $U_{\alpha\beta}$ and $\widehat{U}_{\alpha\beta}(\alpha,\beta=1,2,3)$ are the elements for matrices $\boldsymbol{J}$, $\boldsymbol{U}$ and $\widehat{\boldsymbol{U}}$, respectively, with their explicit expressions shown as follows:

$$
\begin{aligned}
\boldsymbol{J} &= \begin{bmatrix} 1 & -1 & -1 \\ 1 & -1 & -1 \\ 1 & -1 & -1 \end{bmatrix}, \\
\boldsymbol{U} &= \begin{bmatrix} -m_1^{(2)} - \lambda_3^{(2)}(\hat{q}n_1^{(2)} + m_1^{(2)}\hat{r}) & m_1^{(2)^2} + n_1^{(2)^2} - n_3^{(2)}\lambda_3^{(2)}(m_1^{(2)}\hat{q} - n_1^{(2)}\hat{r}) & -\lambda_3^{(2)}[m_1^2 + n_1^{(2)}(n_1^{(2)} - n_3^{(2)})] \\ 1 + \hat{r}\lambda_3^{(2)} & -m_1^{(2)} + \hat{q}n_3^{(2)}\lambda_3^{(2)} & m_1^{(2)}\lambda_3^{(2)} \\ -\hat{r} - \lambda_3^{(2)}(\hat{q}^2 + \hat{r}^2) & \hat{q}n_1^{(2)} + m_1^{(2)}\hat{r} & -\lambda_3^{(2)}[\hat{q}(n_1^{(2)} - n_3^{(2)}) + m_1^{(2)}\hat{r}] \end{bmatrix}, \\
\widehat{\boldsymbol{U}} &= \begin{bmatrix} n_1^{(2)}(1 + \hat{r}\lambda_3^{(2)}) - m_1^{(2)}\hat{q}\lambda_3^{(2)} & n_3^{(2)}\lambda_3^{(2)}(\hat{q}n_1^{(2)} + m_1^{(2)}\hat{r}) & m_1^{(2)}n_3^{(2)}\lambda_3^{(2)} \\ \hat{q}\lambda_3^{(2)} & -n_1^{(2)} - n_3^{(2)}\hat{r}\lambda_3^{(2)} & \lambda_3^{(2)}(n_1^{(2)} - n_3^{(2)}) \\ \hat{q} & -m_1^{(2)}\hat{q} + n_1^{(2)}\hat{r} + n_3^{(2)}\lambda_3^{(2)}(\hat{q}^2 + \hat{r}^2) & \lambda_3^{(2)}[m_1^{(2)}\hat{q} - \hat{r}(n_1^{(2)} - n_3^{(2)})] \end{bmatrix}.
\end{aligned}
\tag{D.3}
$$

Appendix E

$Y_{\alpha\alpha}^{(j)}$ ($\alpha = 1,2,3$, no sum on α) and $\widehat{Y}_{12}^{(j)}$ are expressed as

$$
\begin{aligned}
Y_{11}^{(j)} &= \frac{c_{22}^{(j)}(c_{12}^{(j)} + c_{44}^{(j)})(n_1^{(j)} + n_2^{(j)})}{c_{44}^{(j)}(c_{12}^{(j)} + c_{22}^{(j)}n_1^{(j)^2})(c_{12}^{(j)} + c_{22}^{(j)}n_2^{(j)^2})}, \\
Y_{22}^{(j)} &= \frac{c_{22}^{(j)}n_1^{(j)}n_2^{(j)}(c_{12}^{(j)} + c_{44}^{(j)})(n_1^{(j)} + n_2^{(j)})}{c_{44}^{(j)}(c_{12}^{(j)} + c_{22}^{(j)}n_1^{(j)^2})(c_{12}^{(j)} + c_{22}^{(j)}n_2^{(j)^2})}, \\
Y_{33}^{(j)} &= -\frac{1}{n_3^{(j)}\alpha_{22}^{(j)}}, \\
\widehat{Y}_{12}^{(j)} &= \frac{c_{12}^{(j)}(c_{44}^{(j)} + c_{22}^{(j)}n_1^{(j)}n_2^{(j)}) + c_{22}^{(j)}[c_{44}^{(j)}(n_1^{(j)^2} + n_1^{(j)}n_2^{(j)} + n_2^{(j)^2}) - c_{22}^{(j)}n_1^{(j)^2}n_2^{(j)^2}]}{c_{44}^{(j)}(c_{12}^{(j)} + c_{22}^{(j)}n_1^{(j)^2})(c_{12}^{(j)} + c_{22}^{(j)}n_2^{(j)^2})},
\end{aligned}
\tag{E.1}
$$

for type I roots and

$$
\begin{aligned}
Y_{11}^{(j)} &= \frac{2c_{22}^{(j)}n_1^{(j)}(c_{12}^{(j)} + c_{44}^{(j)})}{c_{44}^{(j)}[c_{12}^{(j)^2} + 2c_{12}^{(j)}c_{22}^{(j)}(n_1^{(j)^2} - m_1^{(j)^2}) + c_{22}^{(j)^2}(m_1^{(j)^2} + n_1^{(j)^2})^2]}, \\
Y_{22}^{(j)} &= \frac{2c_{22}^{(j)}n_1^{(j)}(c_{12}^{(j)} + c_{44}^{(j)})(m_1^{(j)^2} + n_1^{(j)^2})^2}{c_{44}^{(j)}[c_{12}^{(j)^2} + 2c_{12}^{(j)}c_{22}^{(j)}(n_1^{(j)^2} - m_1^{(j)^2}) + c_{22}^{(j)^2}(m_1^{(j)^2} + n_1^{(j)^2})^2]}, \\
Y_{33}^{(j)} &= -\frac{1}{n_3^{(j)}\alpha_{22}^{(j)}}, \\
\widehat{Y}_{12}^{(j)} &= \frac{c_{12}^{(j)}[c_{44}^{(j)} + c_{22}^{(j)}(m_1^{(j)^2} + n_1^{(j)^2})] - c_{22}^{(j)}[c_{44}^{(j)}(m_1^{(j)^2} - 3n_1^{(j)^2}) + c_{22}^{(j)}(m_1^{(j)^2} + n_1^{(j)^2})^2]}{c_{44}^{(j)}[c_{12}^{(j)^2} + 2c_{12}^{(j)}c_{22}^{(j)}(n_1^{(j)^2} - m_1^{(j)^2}) + c_{22}^{(j)^2}(m_1^{(j)^2} + n_1^{(j)^2})^2]},
\end{aligned}
\tag{E.2}
$$

for type II roots.

References

Beom, H.G., Jeong, K.M., Kim, Y.H., 2003. Intensity factors for subinterface cracks in dissimilar anisotropic piezoelectric media. Archive of Applied Mechanics 73, 184–198.

Gao, C.F., Fan, W.X., 1999. Exact solutions for the plane problem in piezoelectric materials with an elliptic or a crack. International Journal of Solids and Structures 36, 2527–2540.

Gao, C.F., Wang, M.Z., 1999. Periodical cracks in piezoelectric media. Mechanics Research Communications 26, 427–432.

Gerasoulis, A., 1982. The use of piecewise quadratic polynomials for the solution of singular integral equations of Cauchy type. Computational Mathematics with Applications 8, 15–22.

Krenk, S., 1979. On the elastic constants of plane orthotropic elasticity. Journal of Composite Materials 13, 108–116.

Liou, J.Y., Sung, J.C., 2007. On the generalized Barnett–Lothe tensors for monoclinic piezoelectric materials. International Journal of Solids and Structures 44, 5208–5221.

Ou, Z.C., Chen, Y.H., 2004. Near-tip stress fields and intensity factors for an interface crack in metal/piezoelectric bimaterials. International Journal of Engineering Science 42, 1407–1438.

Pak, Y.E., 1990. Crack extension force in a piezoelectric material. Transactions of the ASME, Journal of Applied Mechanics 57, 647–653.

Park, S.B., Sun, C.T., 1995. Effect of electric field on fracture of piezoelectric ceramics. International Journal of Solids and Structures 70, 203–216.

Qin, Q.H., Zhang, X., 2000. Crack deflection at an interface between dissimilar piezoelectric materials. International Journal of Fracture 102, 355–370.

Sosa, H., 1991. Plane problems in piezoelectric media with defects. International Journal of Solids and Structures 28, 491–505.

Sung, J.C., Liou, J.Y., 1995a. Analysis of a crack embedded in a linear elastic half-plane solid. Transactions of the ASME, Journal of Applied Mechanics 62, 78–86.

Sung, J.C., Liou, J.Y., 1995b. Subinterface crack in dissimilar orthotropic materials. International Journal of Solids and Structures 32, 2873–2889.
Sung, J.C., Liou, J.Y., 1995c. An internal crack in a half-plane solid with clamped boundary. Computer Methods in Applied Mechanics and Engineering 121, 361–372.
Suo, Z., Kuo, C.M., Barnett, D.M., Willis, J.R., 1992. Fracture mechanics for piezoelectric ceramics. Journal of the Mechanics and Physics of Solids 40, 739–765.
Tian, W.Y., Chau, K.T., 2003. Arbitrarily oriented crack near interface in piezoelectric bimaterials. International Journal of Solids and Structures 40, 1943–1958.
Tian, W.Y., Chen, Y.H., 2000. Interaction between an interface crack and subinterface microcracks in metal/piezoelectric bimaterials. International Journal of Solids and Structures 37, 7743–7757.
Tian, W.Y., Chen, Y.H., 2002. Interaction between subinterface cracks and interface in metal/piezoelectric ceramic bimaterials. Science in China Series E-Technological Sciences 45, 10–18.
Tian, W.Y., Gabbert, U., 2005. Parallel crack near the interface of magnetoelectroelastic bimaterials. Computational Materials Science 32, 562–567.
Ting, T.C.T., 1996. Anisotropic Elasticity: Theory and Application. Oxford University Press.
Ueda, S., 2007. Electromechanical impact of an impermeable parallel crack in a functionally graded piezoelectric strip. European Journal of Mechanics A/Solids 26, 123–136.
Wang, B.L., Mai, Y.W., 2004. Impermeable crack and permeable crack assumptions, which one is more realistic. Transactions of the ASME, Journal of Applied Mechanics 71, 575–578.
Xiao, Z.M., Fan, H., 2001. On the Contact zone and stress singularities of a subinterface crack. Engineering Fracture Mechanics 68 (1), 77–88.
Xiao, Z.M., Fan, H., Sun, Y.M., 2000. On the contact zone of a subinterfacial Zener–Stroh crack. Acta Mechanica 42 (1–4), 133–148.
Yang, P.S., 2008. Analysis of cracked piezoelectric bimaterial with perfectly bonded interface. Ph.D. Dissertation, Department of Civil Engineering, National Cheng Kung University (in Chinese).
Yang, P.S., Liou, J.Y., Sung, J.C., 2007. Analysis of a crack in a half-plane piezoelectric solid with traction-induction free boundary. International Journal of Solids and Structures 44, 8556–8578.